Addis Ababa University

College of Natural and Computational Sciences

Materials science Program

Department of Chemistry

‘Novel Development of Ionic Liquid-based Copolymer Solid Electrolyte for High-Performance All Solid-state Supercapacitor.’

A THESIS SUBMITTED TO A PROGRAM FOR MATERIALS SCIENCE IN PARTIAL FULFILLMENT OF THE REQUIREMENTS FOR THE DEGREE OF MASTER OF SCIENCE IN MATERIALS SCIENCE.

BY: Demelie Yimer Mulatu

ID.No: GSR/6421/13

ADIVISOR: Dr. Girum Ayalneh (Asso.Prof.)

MARCH 2024

ADDIS ABABA, ETHIOPIA

Addis Ababa University

College of Natural and Computational Sciences

Department of Chemistry

Materials science Program

‘Novel Development of Ionic Liquid-based Copolymer Solid Electrolyte for High-Performance All Solid-state Supercapacitor.’

By: - Demelie Yimer Mulatu

Approved by Board of Examiners

Name	Signature	date
Dr. Girum Ayalneh (Asso.Prof.) (Advisor)	_____	_____
Dr. Mekonnen Abebayehu (Asso.Prof.) (Examiner)	_____	_____
Dr.Yedilfana Setarge (Asso.Prof.) (Examiner)	_____	_____

ABSTRACT

In the early 1970s, solid-state materials such as ceramic, glass, crystal, and polymer electrolytes were developed for the purpose of energy storage materials. The energy storage technologies are cutting-edge technologies that are essential for renewable energy, energy management, conservation, and storage, which indirectly contribute pollution control, and greenhouse gas mitigation. Development of solid-state polymer electrolytes (SPEs) is one of the strategies for the development of functional solid-state electrochemical energy storage devices. In this research, polymeric ionic liquid based co-polymer solid electrolytes were synthesized with different ratio of polymeric ionic liquids and copolymers. A simple integration approach enables the quadratic copolymer poly (acrylamide-co-diallyldimethylammonium chloride (PAADDAC) to be well incorporated into chitosan (CS) and polymeric ionic liquid networks during synthesis. Physicochemical characterization techniques such as Fourier-transform infrared (FTIR) and Scanning electron microscope (SEM) were carried out for the spectra analysis of Ionic liquid based Chitosan/Poly (acrylamide-co-diallyldimethylammonium chloride) polymer TFSI (PIL &IL-b-CPE) are based on various chemical crossings. And electrochemical characterization methods such as cyclic voltammetry (CV) and charge discharge of the synthesis membrane were tested. The main emphasis was on materials like conducting copolymer solid electrolytes. Parameters like as energy, capacity, power, cycle performance, and equivalent series resistance are used to analyze the performance of solid copolymer electrolytes. On this solid state SC with ionic liquid impregnation ratio of 25% exhibited the best performance with specific capacitance (Cam) and energy density (Emax) of 3.74 F g-1 and 2.07 Wh kg-1, respectively. These records of worth are only slightly lower than those obtained for convectional SCs using pure TFSI, and much higher as compared with other solid SCs based on conventional polymer electrolytes. This is mainly due to the high electrochemical stability of this PIL &IL-b-CPE that allows these solid SCs to operate at maximum voltages as high as 2 V for the first time.

Keywords:

Supercapacitor, Solid Polymer Electrolytes, Co-polymer Solid Electrolytes, Electrodes

DECLARATION STATEMENT

I, Demelie Yimer, declare that the research project entitled, "Novel Development of High-Performance Ionic Liquid-based Copolymer Solid Electrolyte for All Solid-state Supercapacitor", is my original work that is done under the guidance and advice of my advisor: Dr. Girum Ayalneh (Asso.Pro)

A Thesis Submitted to a program for Materials science in Partial Fulfillment of the Requirements for the degree of Master of Science in Materials science.

This research has not been done before and all sources of materials used for the study have been appropriately acknowledged.

Demelie Yimer ---------- Date 03/03/2024

This Thesis has been submitted for examination with my approval as College supervisor.

ADIVISOR: Dr. Girum Ayalneh (Asso.Pro) …… Date……

ACKNOWLEDGEMENT

First and above all, I would like to praise the almighty God for his help in all effort in my life. I would like to express my deepest appreciation to all those who provided me the possibility to complete this research in one way or another through their prayers, resources and encouragement.

I am very grateful to my advisor Dr. Girum Ayalneh (Asso.Pro) for his professional assistance, patience and understanding that help me for the completion of this research.

I would also like to acknowledge with much appreciation my family, workmates and friends for your encouragement, which has kept me going, and for that am sincerely grateful. It is because of your support that I have managed to get this far, may God bless you abundantly.

TABLE OF CONTENT

LIST OF FIGURES

LIST OF TABLES

LIST OF ABBREVIATIONS

ACs = Activated Carbons

ASCs = Asymmetric Supercapacitors

CD = Charge-Discharge

CNTs = Carbon Nanotubes

COFs = Covalent Organic Frameworks

CPs = Conducting Polymers

CS = Chitosan

Cs = Specific Capacitance

CV = Cyclic Voltammetry

EDLCs = Electric Double-Layer Capacitors

Ed = Energy Density

ESR = Equivalent Series Resistance

ILs = Ionic Liquids

IL-b-CPE = Ionic liquid based Co-polymer Electrolyte

MOFs = Metal Organic Frameworks

PAADADMAC = Poly (Acrylamide-Co-Diallyldimethylammonium Chloride)

PANI = Polyaniline

PIL-b-CPE = polymeric Ionic Liquid Co-polymer Electrolyte

PS–PEO = Polystyrene–Polyethylene Oxide

Pd = Power Density

PVA = Polyvinyl Alcohol

PVDF = Poly-Vinylidene Fluoride

PW = Potential Window

SCPE = Solid Copolymer Electrolyte

SC = Supercapacitor

SCs = Supercapacitors

SEM = Scanning Electron Microscopy

TFSI = Bis (Trifluoromethanesulfonyl) Imide Anion

XRD = X-Ray Diffraction

CHAPTER ONE

1. INTRODUCTION

Electrochemical cells and systems play a key role in a wide range of industries. These devices are innovative technologies that are critical to the application for renewable energy; energy management, conservation, and storage; pollution control; and play a role in reducing greenhouse gas emissions (1–6).

Recent advances in wearable electronics and demonstrations have increased the need to optimize current energy exchange and tidying away technologies. Electrochemical capacitors (ECs) are one of the most important energy storage devices that are receiving a lot of attention due to their high power density, cycle efficiency, and fast charging abilities (3). It stores energy using a charge storage system, EC ion adsorption of electric double-layer capacitors, (EDLCs), or fast and reversible pseudo capacitors. There is another type of capacitor called the "hybrid capacitor" with two different type of electrodes; oneof which is a battery type and the other is a capacitor type (7). A supercapacitor is also called an ultrasound capacitor or electric double-layer capacitor (EDLC). It stores energy in two successive capacitors in the electric field between each electrode and the electrolyte ions. Electricity can be stored directly without a chemical process, so the reaction time is very short. Power densities of supercapacitors are higher compared to those in batteries, but less energy density. Many companies now offer supplier capacitors ranging from 5 F to 2700 F, rated at 2.5 VDC per cell. Single cell storage capacity is 3 or 4 Wh/kg (1–4,6,8). The EDLC has invested heavily in research and development to investigate the two carbon-based electrodes and the organic electrolyte. Undoubtedly, electrolytes play an important role in responsible the performance of ADLCs.

Previous studies have concentrated on liquid electrolytes (LEs) such as water, organic or ionic liquids (9–12). Dissociated salts, which are essentially free ions, make up pure IL. A difference in the ionic concentration between the internal and exterior solutions of the dry gel is created when free ions distribute on the outside of the gel after it is absorbed in pure IL (13,14). Moreover, the collaboration between the polymeric matrix and water was reduced by the effect of IL when the hydrogels were prepared in the IL– water binary system. Environmental risks, corrosion, and

electrolyte leakage are among the flaws that impair LE performance in commercial EDLCs. As a result, it's critical to develop substitute electrolytes for EDLCs. For the aforementioned applications, strong polymer electrolytes (SPEs) are a good option because LEs can have leakage issues and, in a similar vein, demonstrate that capacitors are less dependable and less compact. Despite being more resistive and having a lower melting point than liquid electrolytes, SPE offers ADLC mechanical strength, electrochemical stability, flexible shape, and excellent corrosion resistance (15–17).

However, widespread research struggles on polymer electrolytes have been conducted primarily for H-ion conducting systems (1–7). Moreover, the development of solid-state materials such as ceramics, glass, crystals, and polymer electrolytes began in the early 1970s (18,19). Fenton et al first developed polymer electrolyte in 1973, (19,20). SPEs have been used optimally in fuel cell technology, and some research has been conducted to date on the development of OHIO-average analogs, particularly for ECs (21–23).

In addition copolymers, polymers composed of at least two different types of monomers, can be used as solid electrolytes for solid state electrochemical energy storage devices. Copolymers exhibit better properties compared to monomers, which is related to the relative impact of the integrated structure. The gel PVDF-HPP copolymer showed lower crystallization, lower glass conversion temperature and better solubility in organic solvents associated to PVdF (19). Poly (1-vinylpyrrolidone-co-vinyl acetate) (PVP-co-VAc): This is a copolymer used as a host polymer in gel polymer electrolytes (GPEs). These GPEs play a crucial role in energy storage devices like electric double layer capacitors (EDLCs) and lithium batteries(19). A poly (acrylonitrile-co-methyl methacrylate (P (AN-co-MMA))-based compound, PE, was developed by (EC-PC) as plasticizers. And Lithium Salt ($LiClO_4$) and Silica as Filler. A maximum ion conductivity of 1.9×10^{-3} S cm^{-1} at ambient temperature was obtained with 10 wt.% silica. Possible ionic conductivity due to increased viscosity at plasticizer enrichment. Strong polypropylene electrolyte containing Epichlorohydrin (Epic) is a chemical compound with the formula $C_3 H_5 ClO$, chloride and ethylene oxide shows high ion conductivity at room temperature in KOH systems. The efficacy of epic chloride and ethylene oxide copolymer in electrochemical devices has been tested. This polymer performed well in zinc/air primary cells and nickel/iron hydrated secondary batteries (19,24). (Bei Ao et al., 2017) has published a series of new OH-directed coatings based on chitosan

(CS) and water-soluble quaternary copolymers. For the production of maple electrolytes, CS has been chosen as the polymer matrix because of its high hydrophilicity, excellent film formation, biodegradability, affordability, and non-toxic qualities (25). Furthermore, CS is extremely water-hydrophilic and readily combines with chemical and heat treatment to provide high mechanical strength and chemical resistance because of its abundance of active amino groups (-NH2) and hydroxyl groups (OH). Simultaneously, the use of CS in supercapacitors has been increasingly documented, suggesting its potential use (26,27).

However, the pure CS coating appearances low ionic conductivity with no mobile ions in the structure. Therefore, we use the water-soluble characteristic PAADDA, a catalyst-compliant PAADDA that is compliant with CS and provides ionizers for hydroxide (OH-) as carriers. In chaff preparation, a simple integration method facilitates the smooth integration of the quadratic copolymer PAADDA into CS networks. Thus, interconnecting polymer nets were developed. Phase separation is not necessary to combine the two major solutions because of the strong hydrophilic qualities of CS and PAADDA. Following heat and chemical disintegration procedures, glutaraldehyde (GA) is employed as the binding agent for the coating. Different types of GA CS polymer are formed in the combined process. Specifically, GA discovers two aldehyde groups (CHO) that may be connected to CS through the hydroxyl (-OH) and amino (-NH2) groups. Furthermore, because of its great flexibility, GA outperforms other cross-cutting agents in terms of selectivity and flow (15,26–29). Therefore, the constancy and performance of CS and PAADDA are expected to be significantly improved (30). This thesis review focuses on solid copolymer electrolytes and explores the relevance of electrolytes by reviewing studies in this area. Attempts have been made to estimate their capacity to store more energy than batteries.

1.1. Statement of the problem

The current generation of supercapacitors faces limitations in terms of energy density, power density, and stability, hindering their widespread application in various fields such as portable electronics, electric vehicles, and renewable energy systems. One key challenge is the development of a solid electrolyte that can provide high ionic conductivity, mechanical stability, and compatibility with electrode materials, enabling the realization of all solid-state supercapacitors.

Conventional liquid electrolytes used in supercapacitors have a higher risk of leakage and potential for flammability. They may contain volatile or flammable solvents, which pose safety hazards,

especially in portable electronics or electric vehicle applications. And can have limited stability at high temperatures, leading to a decrease in their ionic conductivity and overall performance. This can restrict their use in applications that require operation at elevated temperatures. Evaporate or dry out over time, which leads to a decrease in their ionic conductivity and performance. This evaporation can limit the long-term stability and reliability of devices utilizing liquid polymer electrolytes.

To address these challenges, this study aims to develop a novel ionic liquid-based copolymer solid electrolyte for high-performance all solid-state supercapacitors. The proposed electrolyte should possess high ionic conductivity, excellent mechanical strength, thermal stability, and compatibility with both electrode materials and the ionic liquid. The development of such an electrolyte would enable the fabrication of supercapacitors with improved energy density, power density, and stability, thereby advancing the field of energy storage technology. The successful development of this novel copolymer solid electrolyte would contribute to the realization of safer, more efficient, and reliable supercapacitors for various applications, leading to advancements in portable electronics, electric vehicles, and renewable energy systems.

1.2. Research objectives

1.2.1. General Objective

The main objective of this work is to synthesis co-polymeric ionic liquid solid electrolytes based on PAADDA, chitosan, GA and ionic liquid electrolytes for high performance solid state supercapacitors.

1.2.2. Specific Objectives

- ♥ To synthesis ionic liquid based Co-polymer electrolytes (PIL&IL-b-CPE)
- ♥ To Prepare carbon electrodes and assembling of solid state super-capacitors
- ♥ To characterize Ionic liquid based Co-Polymer Electrolytes and solid state super-capacitors

1.3. Significance

- Real-time clocks. With appreciate to the long-time backup strength, the standard example is in the real time clocks of electronic systems, which preserve song of the time in

measuring device, control gadget, microcomputer, digital tuning gadget, communique device, and car power supply. Through the usage of EC, endured operation can be guaranteed when the battery is being replaced or eliminated.

- Automobile audio system, taximeter, and emergency lighting. In automobile audio systems and taximeters, EC regularly function the backup for radio station memory, taxi fare applications, and gathered fare information. In emergency lights, EC can electricity emergency lighting for hours inside the event of an energy failure if it is matched with light-emitting diodes (leds).
- Hospitals and medical lifestyles-maintaining gadget. The long predictable lifestyles of EC make it best for hospitals and medical gadget. U. S. A. Systems with EC can offer easy power to shut down safely or trip via for an everlasting primary electricity backup (generally a gas mobile or diesel generator).
- Faraway solar-powered installations or roadside emergency phone. Those structures need dependable backup power to ensure continuous and safe operation in the event of energy failure. Renovation visits to monitor or replace batteries at regular durations are tough and steeply priced. EC is good for these undertaking-critical desks. Three backup software examples of EC supposed use energy supply utility examples of device lengthy-time backup clocks measuring tool, manipulate system, conversation gadgets, car energy resources, microcomputer, static digital tuning device, and so forth. Driving motor, camera, microcomputer microwave oven, microcomputer, memory geared up device, printer, projector, video disk, digital toys, buzzer toys, display tool, alarm tool, actuator, relay solenoid, gas igniter energy assist numerous a power deliver road signal, ups, show light supply: it can be charged for a million times or extra and may preserve appearing reliably without replacement. It could provide bridge electricity to avoid service interruptions until primary backup power assets take over.
- Cameras, programmable pocket calculators, digital agendas, and cell phones. In these appliances, EC can offer energy for seconds to minutes throughout the replacement of the batteries. In video recorders and television satellite receivers, EC is needed to offer electricity backup for length of hours to weeks.
- Flashlights. It can be recharged in a trifling 90 s for every other operation of two h. Meanwhile, it could be cycled for up to 50,000 instances, making upkeep unfastened and

for that reason generating extremely low lifestyles-cycle value. Further, EC can paintings at very-low-temperature environments

1.4. Scope (thematic, spatial, temporal)

The Study was covered the development of high Performance ionic liquid based co-polymer electrolyte and its application in super-capacitor. That is located at Addis Ababa University Natural and computational science college on materials science program laboratory. The key variables that will be covered by the study includes addresses the groundwork of the study. On the basics of ionic liquid based polymer electrolyte, carbon electrodes and assembling of solid-state supercapacitors.

1.5. Limitations of the study

The study is limited to super capacitor of ionic liquid-based Poly (acrylamide-co-diallyldimethylammonium-TFSI) and Poly (diallyldimethylammonium-TFSI) where only experimental. Modeling is presented and for time being computational work is not included. Experimental analysis like FTIR, SEM, FRA, XRF, and charge discharge analysis are used. Origin lab based on version 15 is considered. Due to luck of accessibility of the commercial software, I did not use graph pad prism to the graph of the research.

CHAPTER TWO

2. RELATED REVIEW LITERATURE

2.1. Supercapacitors

Energy is essential to human growth. The global economy and environment are being adversely affected by the energy consumption and production of fossil fuels, which include coal, natural gas, oil, and petroleum. Consequently, there is an increasing need for high-performing, ecologically friendly renewable energy storage devices. Devices for electrochemical energy storage are a crucial component of the pure energy line. Supercapacitors (SCs), fuel cells, and batteries are non-traditional energy sources that function based on the electrochemical exchange of energy. High capacity (CS), extended life cycle, high power density (Pd), low maintenance, memory effect-free, safe, and the energy differential between fuel cells/batteries (large energy storage) and bridge acts (high Pd) (12,33,34). In remote locations without public networks or expensive power lines, these offer a practical solution for rural power provision. Gadgets like cellphones, digital cameras, laptop computers, and mobile gadgets can all be powered by SCs. Supercapacitors were compact, easy to use, and flexible. When braking and providing high Pd for brief acceleration, SCs can be employed in electric and hybrid vehicles to conserve energy and shield batteries from rapid charge (35,36). Traditional capacitors are rigid and bulky and are not suitable for future applications. Thin, light, flexible, clear SCs with many novel features and functions are required for multi-service consumer electronics (12,37,38). Therefore, new materials for SC electrodes such as Covalent Organic Frames (COFs), Metal-Organic Frameworks (MOFs), MXenes, Metal Sulfides, Metal Nitrides, Mixed Heads, 2-D Materials, Ion Liquid Polymer Electrolytes, ion Liquid co-polymer electrolytes, etc., have been synthesized (32,39–43). The small Ed is the key test of tests supercapacitor. Since the energy of the capacitor is directly proportional to the the square of voltage and the capacitance, one of the strategies to increase energy density of supercapacitors is to increase the applied voltage and capacitance. This can be done using electrodes with high conductivities and specific surface area, and electrolytes with a wide electrochemical stability window (ESW). Although the formation of individual components (such as electrodes and electrolytes) of SCs is relatively simple, the correlation between the size of the hole and the structure of the electrolyte ion is

important to promote their synthesized effect. Ionic Liquid-based solid copolymer electrolyte plays an important role in the preparation of important properties such as Pd, temperature, and compact. Other electrolyte requirements for SC are: wide potential window (PW), high ion concentration, good electrochemical stability, low relative resistance (ESR), low variability, low viscosity, non-toxic, low soluble ion radius, and low cost (43).

Classification and operating principles of supercapacitors

Every capacitor exhibitions its exceptional characteristics and applications fluctuating from small adornment applications (normal capacitors) in electronics to high voltage power factor correction applications (supercapacitors) (44).

As shown in the following charts, SCs can be divided into three main categories, based on the charge storage ethics: electric double-layer capacitor (EDLC), pseudo-capacitor (PC), and hybrid supercapacitor (HSC) (45).

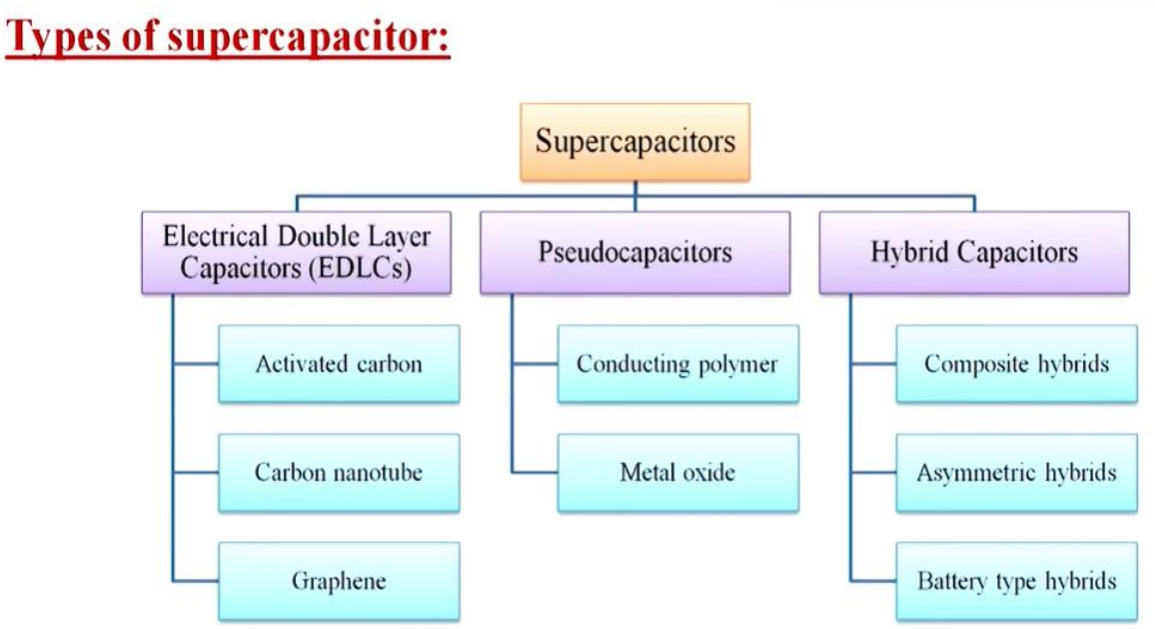

The above associates the power density, energy density, as well as comeback time of each type of SC with Ragone Plot. Some researchers have compared the characteristics of different SCs based on state-of-the art academic research, indicating the difference between their future developments (46).

2.2. Solid-Copolymer Electrolytes

Solid polymeric materials, or SPEs, are able to transport protons, sodium ions, and lithium ions, among other ions. Because of their mechanical and safety qualities, SPEs are thought to be the most viable options for high-performance electrolytes in next-generation power tools (47). Like electrolytes, SPEs are safe. -Enable design flexibility for Organic Light Emitting Diodes (OLEs) and Lithium-Ion Batteries (LIBs). For example, SPEs can support the design of elastic multi-state batteries and micro-electronics micro batteries (48,49). Homogeneous SPEs are pure polymeric solid ion solutions, while different SPEs can be any solid polymeric material with different levels of structure to transport ions. Due to the complexity of polymeric materials, SPEs are often different. A number of factors, including the physicochemical properties of the polymer matrix, determines the three different ion states. Compositions as well as the processing method of SPEs. Therefore, understanding the variability of these levels and the strategies to control them to improve electrolyte properties indicates some important studies for SPEs over the past decade (13,50–52). PEO-based electrolytes are very attractive because they show excellent solubility for lithium salts. In the following, we present a study that focuses primarily on improving SPE ion conductivity based on PEO. Ionic conductivity is the primary property of electrolytes. CE-based SPEs show ion conductivity at room temperature of 10^{-8}-10^{-4} Scm^{-1}, which is less than 10^{-3} Scm^{-1} (typically the required value for practical applications). Therefore, improving ion conductivity is a very challenging and critical issue for SPEs. PEO is a common semi-crystal polymer and can form various compounds with lithium salts due to the bond between Li + and oxygen atoms (53–55). Lithium salts are dissolved by these potent bonding characteristics, but they also serve as anchors to stop ions from migrating. Several facts demonstrate the bonding effects between PEO chains and ions, including the fact that raising molecular weight reduces ion conductivity (56). Plasticizer can dramatically increase ion conductivity, and so on (57,58). The topic of its ability to transport iodine or crystalline ions is still a controversial topic; (59) Therefore, increasing the percentage of PEO electrolyte (amorphous phase) is believed to be one of the most effective ion conductivity methods. Various methods, such as the addition of nanoparticles or plastics and mixing with other polymers, have been used to improve ion exchange. Addition of nanoparticles such as Al_2O_3, (60). SiO_2, (61),and TiO_2, (62) They have been found to be very effective for a number of reasons. First, nanoparticles are additives for the improvement of mechanical properties,

so they can compensate for the mechanical damage caused by low crystallization. Second, nanoparticles can create unique pathways for ion transport in the interphase, further enhancing ion conductivity (63). Copolymer is a candidate for high performance SPEs from conservative blocks (typically PEO blocks) (64). The self-assembled microstructures of copolymer electrolytes, which offer a good compromise between mechanical performance and ion conductivity, are their most intriguing property. Specifically, the ion-conducting PEO block offers a channel for ion transport, and other blocks, such polystyrene (PS) or polyethylene (PE) blocks, provide three-dimensional connected frames with strong mechanical properties. Above importantly, the two blocks can combine to form distinct patterns and channels for the movement of ions. For instance, it has been discovered that PEO-PS electrolyte ion conductivity depends on a certain self-assembled nanostructure, like hexagonal lamellae, by modifying the PEO block fraction in the PEO-PS copolymer and applying flow alignment methods. Parallel lamellae and hexagon-shaped sealed cylinders (64). Although copolymer ions control the Nano-scale pathways for ion transmission, the conduction at the conduction stage is essentially the same as in conventional SPEs, which is usually characterized by copolymer-based SPE ion conductivity. the same as for normal SPEs (65).

2.3. Block Copolymer Electrolytes (BCPE) Overview

Gills and others have reported previous work on BCP electrolytes for lithium batteries. In 1987.24, ethylene glycol methyl ether (MPEG) was installed on the polybutadiene block of a poly (styrene-b-butadiene-b-styrene) (PS-PB-PS) Triblock block-polymer (PS-P (B-g). -MPEG)-PS) graft copolymer. Except for the low doping ratio ([EO]: [Li] 550: 1), these $LiCF_3SO_3$-doped PS-P (B-g-MPEG)-PS molecules with different MPEG lengths and salt concentrations were molecules at the temperature studied.(66,67). The maximum ion conductivity obtained at 20 °Cis about 1025 S/cm. Later, in 1989, Khan et al. reported the ABA triblock copolymer electrolyte system reported by PS Medium block and POEM-PS-POEM. /cm at 25 °C for [EO] [$LClO_4$] 17:11 ratio. However, morphological and mechanical analyses have not been reported in the works of Gills or Khan's. Over the past decade, salt doping BCPE has attracted more interest in its mechanical and morphological properties, and several studies have shed more light on the impact of salt doping on ionic conductivity, mechanical strength, and morphology (68). These studies have shown that the prescribed BCPE system is more effective than related random copolymers, dissociated BCPEs, and homo-polymers (69). e.g., (styrene-g-ethylene oxide) -b-styrene (PS-P (S-g-EO)-PS) Tribble

block copolymer (contained in a copolymer, with 60% weight portion) exhibited an elastic modulus of -109 dyn/cm^2 between 0 and 100 ^{0}C, which was much higher than the equivalent elastic modulus of PEO homo-polymer electrolytes). This elastic modulus was close to the shear modulus required to inhibit macroscopic dendrite formation (estimated by Monroe and Newman at -7 GPa23) and therefore protect the battery from short circuits. Furthermore, the copolymer electrolyte ion conductivity for this stroke is 2 x 10^{-5} s/cm at room temperature. (At 60 ^{0}C, this is also 10 - 4 S/cm.) 80% in recent years, PS-PEOs have become the most attractive candidates for BCP electrolytes due to their attractive performance in batteries. PS-PEO systems at 1023 S/cm ([Li]/ [EO]) and 81 and 108 Pa at 90 °C. At densities of 27 and 1023 S/cm ([Li]/ [EO]), ion conductivity can be achieved. After 300 cycles, PS-PEO electrolytes showed good cycle life at 90 °C and an electrochemical stability window up to 3.7 V at 80% of their initial capacity. Application of PS-PEO electrolytes is restricted. Although the current modulus of most BCP electrolyte systems is less than 7 GPa, conductivity and mechanical strength are depleted in BCPs, thus allowing them to increase their ability to reduce sliding modules in the future. In this work, we aim to provide an overview of ion conduction for supercapacitors filled with BCP electrolytes and refer readers to additional sources on battery performance (70–72).

2.4. Properties of heterogeneous electrolytes

It is recommended to employ a variety of polymer electrolytes with and without ion-rich areas in the majority of practical applications. The conductivity of heterogeneous electrolytes, σh, can be obtained in the simplest approximation by:

$$\sigma h = f \varphi c \sigma c \qquad (1)$$

Where f denotes the executive level's strength and relevance, φc is the executive phase's volume proportion, and σc represents intrinsic conductivity. According to Equation 1, there is no ion transport in the electrolyte ion-poor areas. The conducting phase is the minor component in micro phase-separated block copolymers, and Table 1 displays the optimal morphological factors for 1D transport.

Table 1 : Ideal morphology factors for 1D transport in micro phase-separated block copolymers

Morphology	***F* ideal**
Gyroid	1
Lamellar	2/3
Cylinders	1/3
Spheres	0

Electrolyte, σh, is given by

$\sigma h = f\sigma c$,

Take note that Equation 1 does not contain φc. Within this assumption, we anticipate that the transference numbers of the homogeneous and heterogeneous electrolytes will be equal. Self-assembling ionic and nonionic block copolymers is the best method for producing various electrolytes (68,73–75). The most common morphological units in these systems are alternate lamellae, gyroid networks, hexagonal cylinders, and cube-shaped spheres. We describe the exact morphological state that is found in the absence of faithful, tragic paths and dead ends (63). 2/3 of the fidelity is to changing and directing the lamps, following the well-known methods of transport in various media. The matrix is 1/3, and it is faithful to lead in a matrix that does not lead to spheres.

It is fideal 1 if the nonlinear phase is the smallest component (such as the defenses in the matrix that direct the cylinders). A summary of pertinent morphological factors can be found in Table 1. Table 1 lists the transport characteristics of a few chosen heterogeneous polymer electrolytes. The properties shown in Table 1 are \c; h; D; Faithful; f; which is defined by the conductive parameters; and C, which is computed assuming that all ions are in the leading domains and accounting exclusively for the size of the lead. The t + parameters in various electrolytes are unknown to us. Supplement Table 1 contains a thorough explanation of our methodology for determining the parameters in Table 3. First, the PS-PEO block polymer with LiTFSI is the input in Table 3. The type III electrolyte in this instance is the lead stage. In terms of lamellar morphology, PS-PEO/LiTFSI electrolytes behave well up to the highest molecular weight limit, i.e., f = fideal, σc = σ, and Dc = D (in experimental error). When used with PEO cylinders, PS-PEO/LiTFSI

electrolytes exhibit poor behavior. It is found that f has a value of 0.13, which is not very trustworthy. The internal efficiency of the leadership level (C = σ) is altered by nanoscale restrictions and resistance to grain boundaries, which are the two factors contributing to negative behavior. Polystyrene-block poly (ionic liquid)] (PS-PIL) is the second input in Table 1. An electrolyte of the IV type is the lead stage. F is significantly less than fide for lamellar and cylindrical morphologies. Leadership level discrepancies could be the cause of the discrepancy in f value observed in the lamellar levels formed in PS-PEO and PS-PIL. The obvious historical differences in various laboratories could also be the cause of the variation in the f value found for the two polymer electrolytes. The wet PSS-PMB block polymer—PSS-PMB stands for polystyrene sulfonate-block-poly—is the third input in Table 1. This lead stage is an example of a V electrolyte. Compared to other electrolytes of type III or type IV lead, these electrolytes have a significantly higher activity. The primary cause of this discrepancy is the effectiveness of proton transport in water. The relationship between σc and σ is not evident; however the aforementioned framework should be used to this polymer in order to measure the difference between σh and σh. Stated differently, it is unclear which electrolyte should be utilized in order to understand σh readings. Furthermore, it is unknown what value φc is in Formula 1. We assumed that the lead level in the PSS-PMB analysis is PSS / H2O and that H2SO4/H2O is a reasonably equivalent electrolyte with an H+ molar focus, c, of 0.44 Mol. liter-1. At a relative humidity of 98%, the water content of the particular PSS-PMB polymer is 0.82 g per gram of polymer, resulting in φc = 0.91 (60). Using Equation 1, we obtain f = 0.77. The hybrid polymer morphology is lamellar, and therefore the fidelity is 2/3. The f and faithful values of this system are in harmony with each other. We have made many simple assumptions for discussion. One might calculate, for example, in the PSS-PMB copolymer by dividing the H + molecules into water samples, i.e., not counting the presence of PSS in the lead channels. As a result, the value of c is 0.49 Mol. liters^{-1}, which is not much different from the 0.44 Mol. liters^{-1} estimate (47).

2.5. **Electrochemical** Capacitors

Related electrochemical energy-storage devices are batteries and electrochemical capacitors. But an EC's charge-storage mechanism—which is usually capacitive rather than faradaic—sets it apart from a battery. While reversible ion adsorption takes place at the electrode surface for a capacitive process during charge and discharge, the faradaic process involves redox reactions at the anode

and cathode (76). There are two types of capacitors: (i) electrolytic capacitors and (ii) electrochemical capacitors (ECs), which include electrochemical pseudocapacitors and electric double-layer capacitors (EDLCs). An EDLC, on the other hand, refers to double-layer charging at a high-surface-area electrode, usually carbon. An electrolytic capacitor stores energy by charge-separation across a thin insulating dielectric oxide layer.

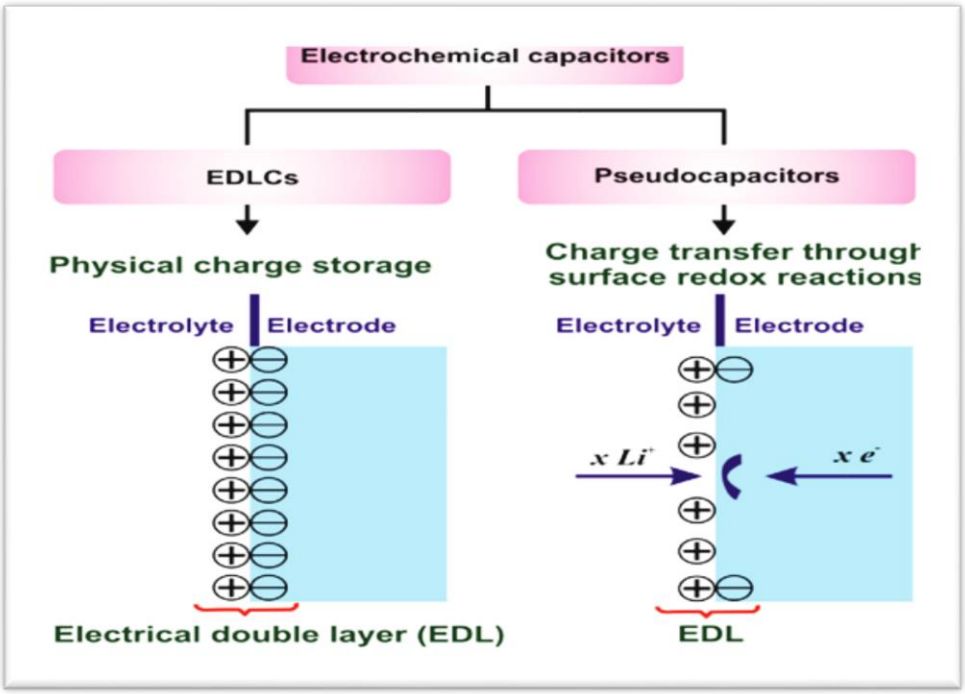

Figure 1 Classification of electrochemical capacitors. EDL, Electrical double layer; EDLCs, Electrical dual layer condensers (76).

The typical components of a carbon-based electrochemical cell (EC) are two thick carbon films acting as the positive and negative capacitive electrodes in contact with a suitable current collector and an electrolyte, which can be an ionic liquid or an aqueous or nonaqueous solution (Fig. 1). The charge separation at the solid/liquid interface between the carbon and the electrolyte is essential to the processes that make up the charge-storage mechanism. In the less complicated scenario, the positive charge that accumulates in the positive carbon electrode during charging is offset by anions from the electrolyte. Finally, another sort of EC is based on the active electrode's capacitive charge and faradaic pseudo capacitance. In a similar manner, the negative charges existing in the negative electrode following charging are compensated by cations from the active material. This class encompasses redox processes in conducting polymers and metal oxides.

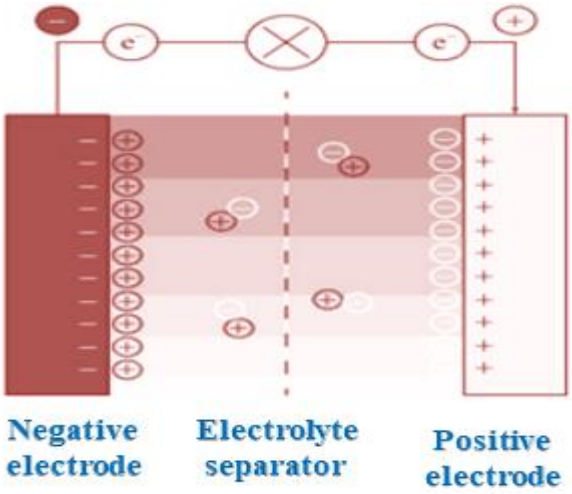

Figure 2 graph of negative electrode, electrolyte separator, and positive electrode

Negative electrode separator Separator of electrolytes a positive electrode Figure 2 Diagram showing the operation of an electrochemical capacitor with two carbon electrodes, an electrolyte, and a membrane present. With an excess of charge in each electrode that is offset by ionic species with the opposite charge, the capacitor is shown in its charged condition.

2.6. Electrochemical characterization of all-solid state supercapacitors

Cyclic voltammetry (CV); a powerful technique used to investigate electrochemical processes that has been attracting much attention in relation to renewable energy. CV studies provide information about (1) the formal potential and its close link to the standard reduction potential of redox couples, (2) the charge-transfer kinetics of electrodes, (3) the concentration of redox couples, (4) chemical reaction mechanisms, and (5) the diffusion coefficient of redox couples, among others (88).

CHAPTER THREE

3. RESEARCH DESIGN AND METHODOLOGY

3.1. Research Design

3.2. Research Methods and procedure

3.2.1. Materials

Chemicals

Lithium bis(trifluoromethanesulfonyl)imide (LiTFSI, 99%) and N-Methyl-N-butylpyrrolidinium bis(trifluoromethanesulfonyl) imide. Poly (diallyldimethylammonium) chloride solution (pDADMAC) (average Mw 400,000 - 500,000, 20% wt. in H2O) was obtained from Aldrich. Poly (acrylamide-co-diallyldimethylammonium chloride) solution (PAADDA) (10% wt. in H_2O) was obtained from Aldrich. Acetic acid (25%), Chitosan, Glutaraldehyde, Acetone (purity >99.5%) will use for the preparation of the electrolyte solution. Distilled water, polytetrafluoroethylene (PTFE), Activated charcoal.

Apparatus

a) Digital Balance
b) magnetic stirrer with hot plate,
c) Metrohm Autolab PGSTAT
d) universal hot air Vacuum Oven
e) FTIR Spectrometer
f) coin shape current collector puncher
g) butchener funnel
h) distiller
i) Swalog apparatus

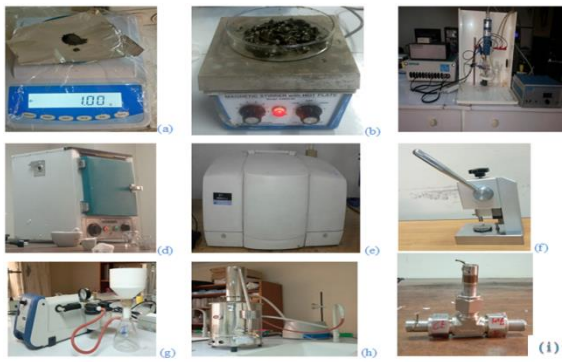

Figure 3 : List of apparatus

3.2.2. Synthesis and preparation of polymer ionic and ionic liquid based Copolymer electrolyte (PIL&IL-b-CPE)

a) Preparation of Il-b CPE

As starting materials a, 0.67: 0.33 ratio of CS: CPE which was mixed according to (15). As a linker, 80 micro liter of Glutaraldehyde (GA) solution in 2% of acetic acid was added and prepared and the solution was kept for the ionic liquid based copolymer electrolyte (IL-b-CPE). For the preparation of IL-CPE, different weight ratio of ionic liquid, N-Methyl-N-butylpyrrolidinium bis (trifluoromethanesulfonyl) imide (TFSI) and CS&CPE mixture were mixed together. On the base of previously synthesized of 0.67: 0.33 ratio of CS: CPE prepared ratios of CS&CPE and TFSI solution were (1: 0.1, 1: 0.17, 1: 0.2 and 1: 0.25 by weight) (CS/PAADDA-OH^-: TFSI).

b) Synthesis of PIL-b-CPE

The ionic liquid based polymer electrolyte polymeric ionic liquid (PIL) was prepared by dissolving 1.4 g of PIL (PDADMATFSI) in 4 ml of acetone and the mixture was stirred with magnetic stirrer until it completely disolves (32). Instead of addition of pure IL solution in to the CS-CPE mixture, different ratios of PIL were added into the mixtures of CS-CPE. The solution was named as PIL-b-CPE and the prepared ratios were (1: 0.1, 1: 0.17, 1: 0.2 and 1: 0.25 by weight).

c) Synthesis of PIL-b-CPE and IL composite

Finally, For the preparation of PIL&IL-b-CPE, different weight of N-Methyl-N-butyl pyrrolidinium bis(trifluoromethanesulfonyl)imide (TFSI) was added to the mixture of PIL-CPE. The prepared ratios were (1: 0.06, 1: 0.1, 1: 0.12, 1: 0.15 and 1: 0.18 by weight) (PIL-b-CPE: TFSI). Relatively the optimum amount of physicochemical and electrochemical parameters the selected ratio was 1: 0.15 by weight) (IL-b-CPE: TFSI) for solid-state co-polymer electrolyte of supercapacirors.

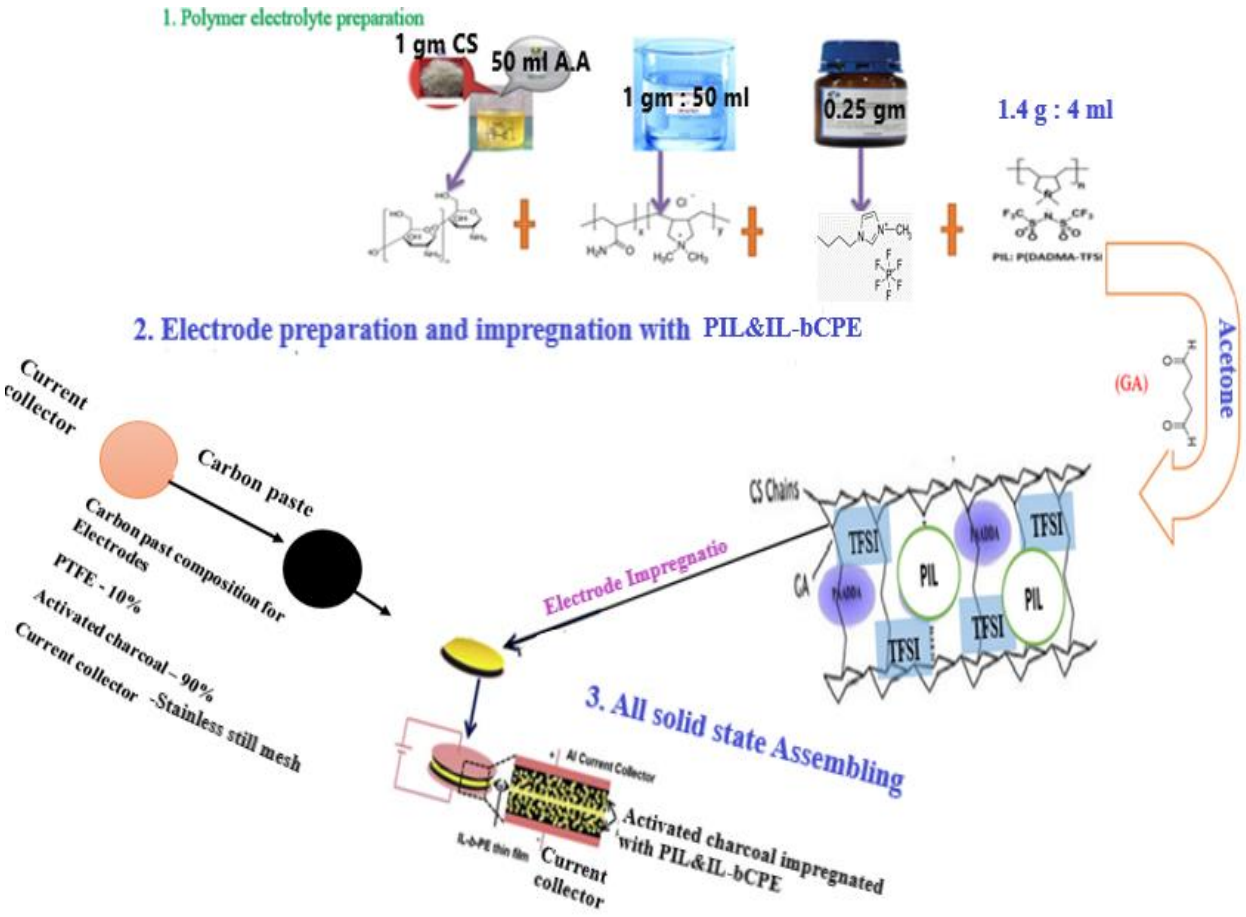

Figure 4 : Synthesis and preparation of ionic liquid based Copolymer electrolyte (IL-b-CPE)

Source: (15,32)

The impregnated electrode would then dry at ambient °C under vacuum overnight before characterization.

3.2.3. Preparation of carbon electrodes

Activated Charcoal being the active material, Activated charcoal and PTFE (90:10) was mixed in beaker land until the homogeneous carbon paste was obtained. Carbon electrodes were prepared by rolling the carbon paste on the stainless still mesh current collector (0.9 mm diameter and 99% purity). Finally, the electrodes were dry at 80 °C overnight. The final carbon electrodes had a thickness of approximately about 17 – 20 mm.

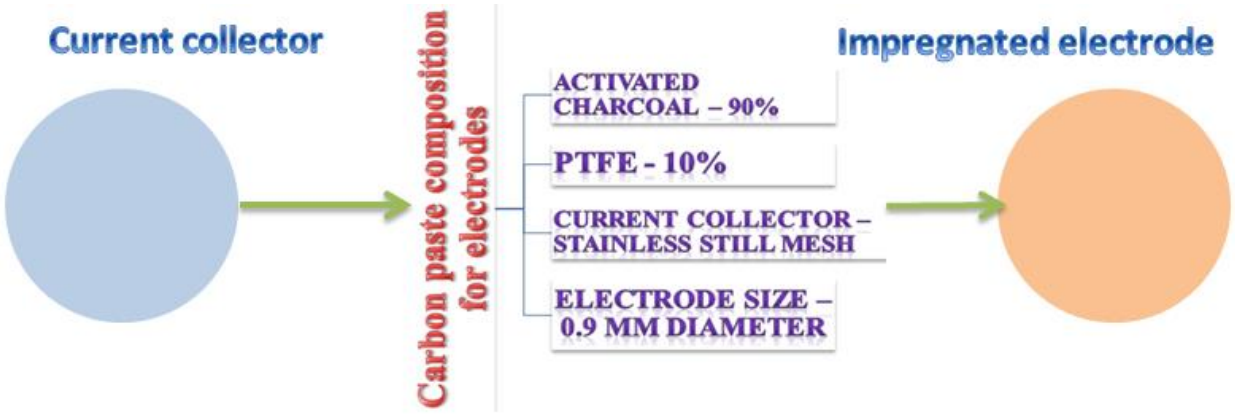

Figure 5 : electrode preparation

3.2.4. Electrode impregnation and all-solid state super capacitors assembling

Using a micropipette, the diluted acetone PIL&IL-b-CPE solution was added to the porous carbon electrodes to impregnate them. To create electrodes with varying PIL&IL b-CPE to active material ratios (starting at 1.00 by weight), varying volumes of PIL&IL-b-CPE solution (ranging from 20 ml to 80 ml) were added. The porous carbon electrode allowed the PIL&IL-b-CPE solution to spread quickly, which allowed the carbon electrode's particles to become filled with PIL&IL-b-CPE. To ensure a smooth impregnation, the impregnated electrodes were processed for one hour while under vacuum. The impregnated electrodes were then left to dry overnight in a vacuum at room temperature. In the end, two impregnated electrodes with identical active mass and impregnation ratio were faced in a two-electrode Swagelok cell to create all-solid state polymer electrolyte super capacitors. There was no need to put an extra separator between two electrodes because the PIL&IL-b-CPE layer on the electrode surface served as both a solid electrolyte and a separator. This is undoubtedly one of these solid state SCs' advantages. A variety of SCs were constructed with varying PIL&IL-b-C PE to active mass ratios.

3.2.5. Characterization Procedures of physico-chemical Supercapacitors

3.2.5.1. Fourier-transform infrared (FT-IR)

Fourier-transform infrared (FT-IR) spectra were recorded on an FTIR-4200 spectrometer (Shimadzu) with a wavenumber resolution of 4 cm^-1 in the range 400 - 4000 cm^-1. Samples in the form of thin films were sandwiched between two KBr plates and placed in the cell to be measured. Air was employed as a background reference

3.2.5.2. Scanning Electron Microscopy (SEM)

The composite morphology was inspected using SEM, JCM-6000 Plus field-emission scanning electron microscope (SEM) operating at 5 kV. Prior to explanations, the membrane samples were splintered in liquid nitrogen and examined from (20 μm - 500 μm) × magnification.

3.2.6. Characterization Procedures of Electrochemical Supercapacitors

3.2.6.1. Cyclic Voltammetry

Potentiostat measurements were used to assess the electrochemical stability windows of the PIL&IL-b-CPE at 5 to 50 mV s-1. The measurements were conducted using a stainless steel electrode/current collector with a polytetrafluoroethylene separator shaped like a ring, the ionic liquid placed in the center, and an Ag wire inserted into the sample as a pseudo-reference. Cyclic voltammetry (CV) was used to assess the supercapacitors' (SC) electrochemical behavior. The SC was subjected to cyclic voltammetry (CV) tests using two electrode configurations to examine the cell's performance at various voltages and three electrode configurations to assess the electrochemical behavior of the positive and negative electrodes independently within the potential ranges identified by the galvanostatic experiments. The CV tests in the three-electrode configuration were performed using Cu wire as the counter electrode and an Ag wire as pseudoreference electrode.

3.2.6.2. Galvanostatic Charge-discharge

The electrochemical stability windows of the PIL&IL-b-CPE were evaluated by carrying out Potentiostat measurements, using a stainless steel electrode/current collector with PIL and IL based copolymer electrolyte in the middle and with an Ag wire inserted into the sample as a pseudo-reference. The electrochemical manner of the supercapacitors (SC) was evaluated by galvanostastic tests. The galvanostatic tests were performed at different current densities (0.1 - 0.5 mA cm^-2 in relation to the active mass of the electrodes) and at different voltages. To enable the simultaneous recording of the cell voltage and the potential of each electrode, the cells were built utilizing an Ag wire as a pseudo-reference electrode. A Potentiostat/Galvanostat instrument was used for every electrochemical measurement, and it was kept at room temperature. Based on the galvanostatic curves and the reference provided, the following values were determined: cell

capacitance (Ccell), energy density (E), power density (P), and equivalent series resistance (ESR) (details of the calculations can be found in Supporting Information) (77)**.**

From the CD experimental data, specific capacitance (C_{sc}), equivalent series resistance (ESR), maximum energy (Emax), maximum power (Pmax) and real specific energy (E_{real}) for full supercapacitor will calculate as shown below.

$$C_{SC}(Fg^{-1}) = \frac{I}{m_{tam}.\frac{dv}{dt}} \quad (1)$$

$$ESR(\Omega cm^2) = \frac{\Delta V.A}{2.I} \quad (2)$$

$$E_{real}(whkg^{-1}) = \frac{I}{m_{tam}} \int_{t_i}^{t_f} V dt \quad (3)$$

Where I is the discharge current, M_{tam} is the supercapacitor's total active mass (the mass of Pica carbon in both electrodes), dV/dt is the discharge curve's slope, dV is the ohmic drop when the current is reversed, and A is the electrodes' geometric area. The integration limits, ti and tf, are the times at which discharge begins and ends, respectively. The specific capacitance of a single electrode (Cam) in a symmetrical system is connected to the capacitance of the SCs (CSC) using the following expression:

$$C_{am}(Fg^{-1}) = 4C_{SC} \quad (4)$$

$$C = \frac{Q}{\Delta Em} \quad (4.1)$$

Constant current charge–discharge curves (Fig. 13) can also be used to evaluate the specific capacitance of a single electrode by using

$$C = \frac{It_d}{\Delta Em} \quad (4.2)$$

Where ΔV is the potential decrease during constant current discharge, td is the discharge period, and I is the total current. Alternatively, by dividing the discharge current (I) by the slope of the discharge ((dv^{s}$_{T}$$_{x}$dt)in V/s) curve, the capacitance can also be determined.

$$C = \frac{I}{(dv|dt)} \quad (4.3)$$

It should be noted that the discharge curve of an ideal electrical double-layer capacitor typically has a slope, whereas the discharge curves of batteries typically have plateaus. Determining the capacitance of the two-electrode EC is more pertinent, even though the precise capacitance values of a single electrode are frequently reported and offer a convenient means to evaluate the performance of different EC materials.

CHAPTER FOUR

4. RESULTS AND DISCUSSION

4.1. Physicochemical characterization

4.1.1. FT-IR analysis

The typical FT-IR spectra measured for PIL&IL-b-CPE are shown in Fig. 6, along with an identification of their various constituents. Furthermore, FT-IR analysis was performed on the freestanding membranes following chemical cross-linking alterations. The strong band seen in all of the spectra between 3300 and 3500 cm-1 is mostly ascribed to the stretching vibration of the -OH groups in chitosan or potentially bound ambient water during the polymer production process. Because of PAADDA's hydrophilic impact, the peak intensities of PIL&IL-b-CPE membranes with GA as an organic linker were significantly higher than those of the CS/CPE membrane. The -CH3, -CH2, and -CH groups are stretched, resulting in the bands at 2925 and 2886 cm-1. The occurrence of cross-linking in the CS membrane has been proven by IR amounts, where the appearance of a high-pitched absorption band at 1640 cm^{-1} (C=O) was saw due to the 'free' -CHO attached to GA (78,79). Furthermore, the cross-linking network between CS and GA is most likely what is responsible for the amplification of the C-O-C ester mode at 1192 cm-1. Furthermore, there is a significant increase in the peak intensities of (C=O) and (C-N) at 1640 cm-1 and 1055 cm-1, respectively, when the TFSI content increases. These outcomes unequivocally demonstrate that the quaternary ammonium groups were successfully incorporated into the PIL&IL-b-CPE membranes. This suggests that a higher network density results in less accessibility to the reactive groups. Furthermore, as the amount of IL grew, the peak intensities of both amides increased noticeably, demonstrating that IL was successfully incorporated into the polymer matrix.

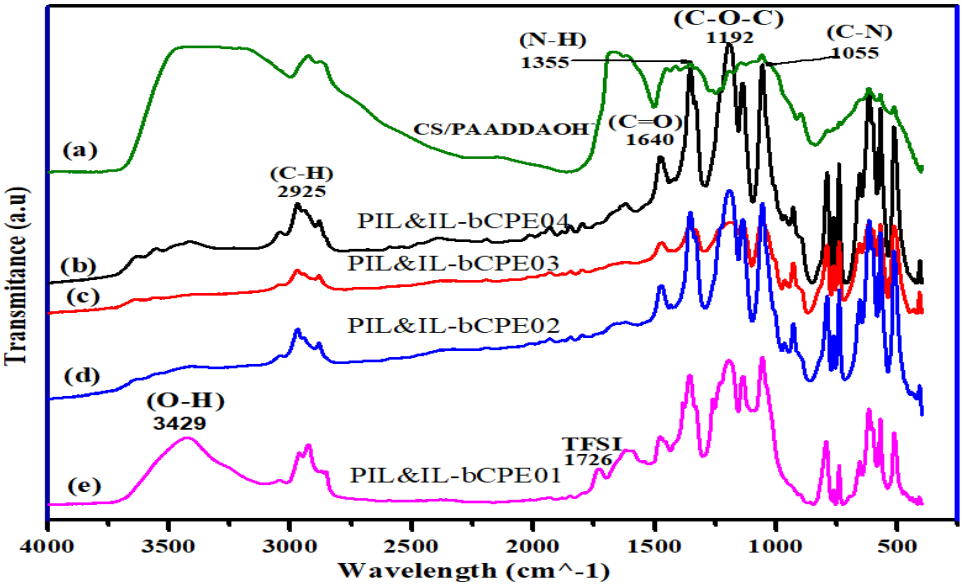

Figure 6 : FTIR spectra of chemically cross-linked PIL&IL-b-CPE membranes.

(a) CS: PAADDA-OH= 0.67:0.33 by weight, (b) PIL-b-CPE: TFSI = 1:0.06, by weight, (c) PIL-b-CPE: TFSI = 1:0.1 by weight, (d) PIL-b-CPE: TFSI = 1:0.12 by weight, (e) PIL-b-CPE: TFSI = 1:0.15 by weight

4.1.2. SEM Analysis

The PIL&IL-b-CPE composite membranes are all translucent with a white color; Fig. 7 displays a typical sample of one of these membranes. Fig. 7 summarizes the cross-sectional SEM images of these membranes. Every PIL&IL-b-CPE membrane often exhibits a rough surface and a dense structure. The self-stand membrane picture (Figures 7c and d) demonstrates the surface appearance of several areas that suggest micro-phase separation during the mixing of the various composite polymer components. This is especially detrimental to continuous ion conduction and the stability of the resulting device, and it suggests that, in contrast to the findings we published in, CS, PAADDA, PIL, and TFSI are not effectively mixed with GA as the cross-linking reagent (32). It's noteworthy to note that these membranes differ significantly from those developed before for anion conducting membranes using chitosan and poly(acrylamide-co-diallyldimethylammonium chloride) (15). This study shows that PAADDA is tightly trapped into the CS polymer matrix, forming a dense network; nevertheless, because of the positive charge of the quaternary ammonium groups on PAADDA, a partial incompatible condition arises between greater levels of PAADDA, PIL, TFSI content, and CS, resulting in a stiff structure.

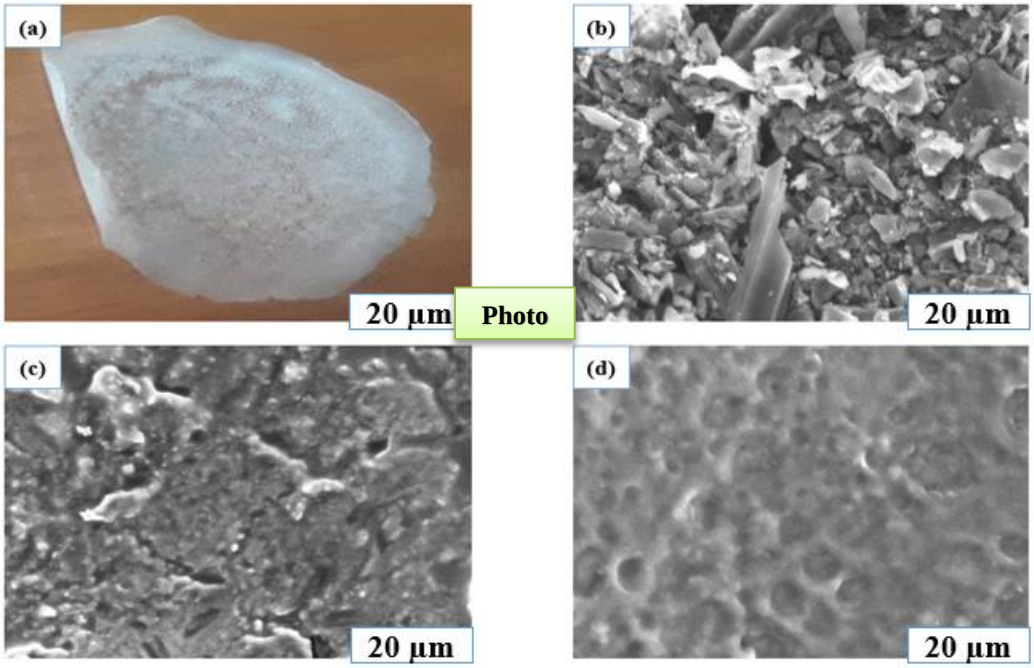

Figure 7 : SEM image of (a) photo of self-stand electrolyte, (b) Carbon paste electrode, (c) Impregnated of carbon paste electrode, (d) polymer electrolyte self-stand membrane.

4.2. Electrochemical characterization of all-solid state supercapacitors

4.2.1. Cyclic voltammetry

The analysis of a supercapacitor cyclic voltammetry (CV) graph can provide valuable information about the capacitance, performance, and characteristics of the supercapacitor. Here are some steps to analyze the graph:

Determine the shape of the CV curve: A symmetric and rectangular shape indicates an ideal capacitive behavior. Calculate the specific capacitance: This can be done using the formula C = (I* AV) / (m* At * AV), where I am the current, AV is the potential window, m is the mass of the active material, and At is the time period. Analyze the voltage drop: A large i voltage drop indicates a higher internal resistance, which may affect the performance of the supercapacitor. Look for any redox peaks: These indicate the presence of faradaic reactions, which can affect the stability and lifespan of the supercapacitor. Compare the CV curves at different scan rates: The specific capacitance should remain constant at different scan rates, indicating good rate capability.

The area enclosed by the CV curve proportional to the specific capacitance of the supercapacitor. The larger the area, the higher the capacitance. The slope of the CV curve during the linear region

indicates the diffusion coefficient of the electrolyte ions. A higher slope corresponds to a faster diffusion rate. The stability of the supercapacitor can be assessed by comparing the CV curves over multiple charging and discharging cycles. Any significant changes in the curve shape or specific capacitance may indicate degradation. The peak-to-peak separation (AE) in a CV curve can be used to estimate the charging time of the supercapacitor. A smaller AE corresponds to faster.The presence of satellite peaks in t. CV curve may indicate the presence of side reactions or impurities, which can affect the supercapacitor's performance and stability.

a. CV of IL-b-CPE

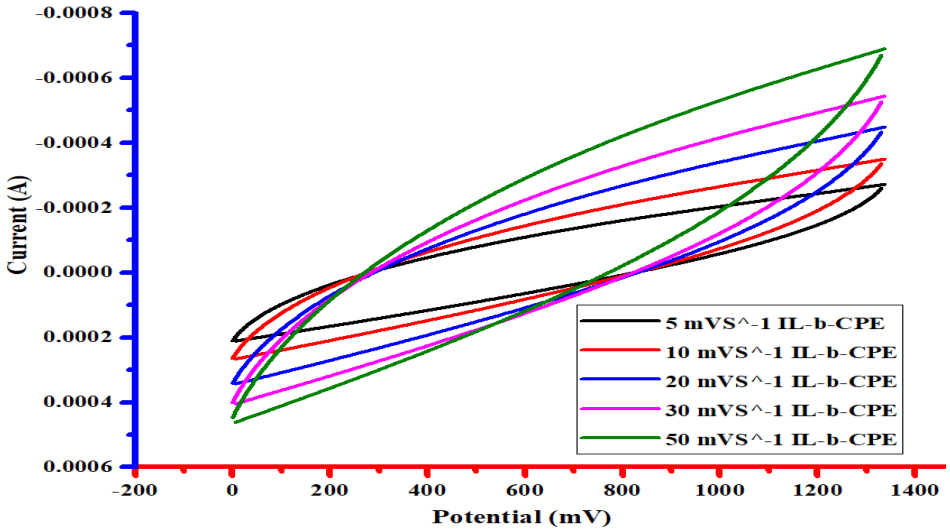

Figure 8 : CV graph of 3 scan of 5-50 mVS^-1 IL-b-CPE

The power delivered by the supercapacitor is given by the formula P = I * V, where I is the current and V is the voltage. In this case, the power is P = (-0.5 mA) * (1.3 V) -0.65 mW. Since the power is negative, it indicates that the supercapacitor is discharging. Energy Storage and Discharge: The energy stored in a supercapacitor is given by the formula E = (1/2)* C * V^2, where C is the capacitance. Given the voltage of 1.3 V and the current of -0.5 mA, we can calculate the capacitance using the formula I = C * (dV/dt). Solving for C, we find C = (2 * I) / (dV/ dt). Plugging in the values I = -0.5 mA and dV/dt = 1.3 V/20 s (assuming a 0.065 F. Now we can calculate the energy stored in the supercapacitor: E ≈ (1/2)* 0.065 F* (1.3 V) ^2 ≈ 0.055 J. This energy will be dissipated during the discharge process.

Impact on Performance: The discharging of the supercapacitor will affect its performance in terms of the available power and the time it can supply the load. In this case, the supercapacitor can

supply a load of -0.65 mW for a certain period, depending on the specific application and discharge voltage threshold. 4. Comparison with Other Energy Storage Devices: Comparing the energy storage and discharge characteristics of the supercapacitor with those of other Supercapacitor with those of energy storage devices, such as batteries, can provide insights into the relative performance of the two technologies for specific applications.

b. CV of PIL-b-CPE

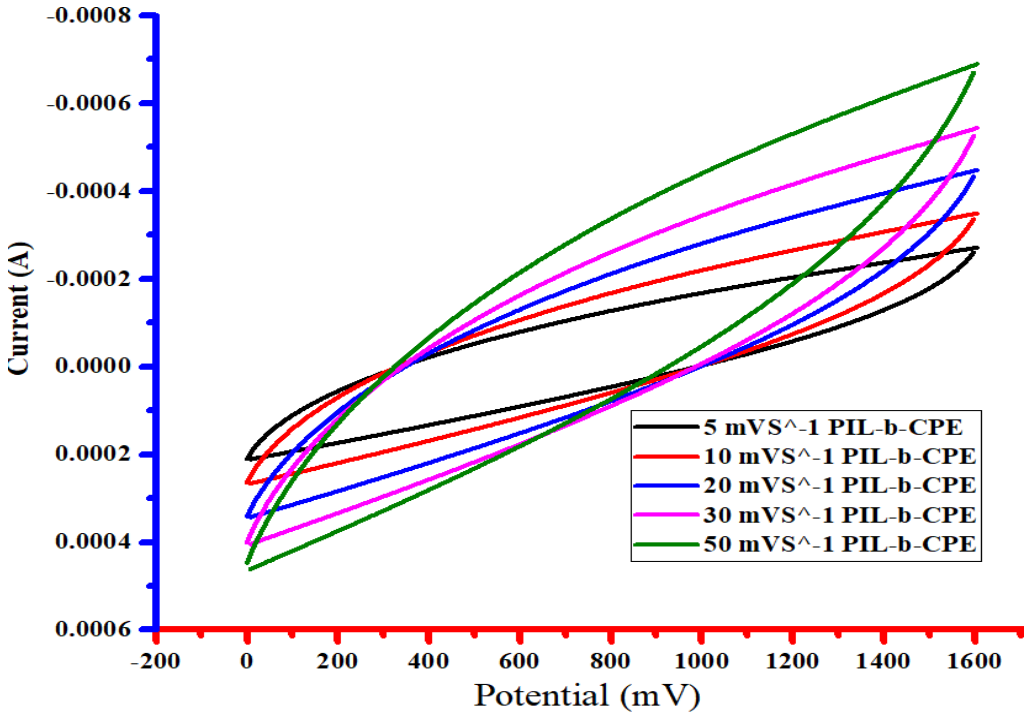

Figure 9 : CV graph of 3rd scan of 5-50 mVS^-1 PIL-b-CPE

Given the change in energy of 1.6 V & a current of -0.5 mA, we can discuss the following aspects related to the charging or discharging of a supercapacitor:

Energy and Power: The power delivered by the supercapacitor is given by the formula P = I* V, where I is the current and V is the voltage. In this case, the power is P = (-0.5 mA) * (1.6 V) = -0.8 mW. Since the power is negative, it indicates that the supercapacitor is discharging.

Energy Storage and Discharge: The energy stored in a supercapacitor is given by the formula E = (1/2) * C * V^2, where C is the capacitance. Given the voltage of 1.6 V and the current of -0.5 mA, we can calculate the capacitanc using the formula I = C * (dV/dt). Solving for C, we find C

= (2 * I) / (dV/ dt). Plugging in the values I = -0.5 mA and dV/dt = 1.6 V/20 s (assuming a 20-second charging scenario), we get C ≈ 0.08 F. Now we can calculate the energy stored in the supercapacitor: E (1/2) * 0.08 F* (1.6 V) ^2 ≈ 0.102 J. This energy will be dissipated during the discharge process.

Impact on Performance: The discharging of the supercapacitor will affect its performance in terms of the available power and the time it can supply the load. In this case, the supercapacitor can supply a load of -0.8 mW for a certain period, depending on the specific application and discharge voltage threshold.

Comparison with Other Energy Storage Devices: Comparing the energy storage and discharge characteristics of the supercapacitor with those of other energy storage devices, such as batteries, can provide insights into the relative performance of the two technologies for specific applications.

c. PIL & -b-CPE

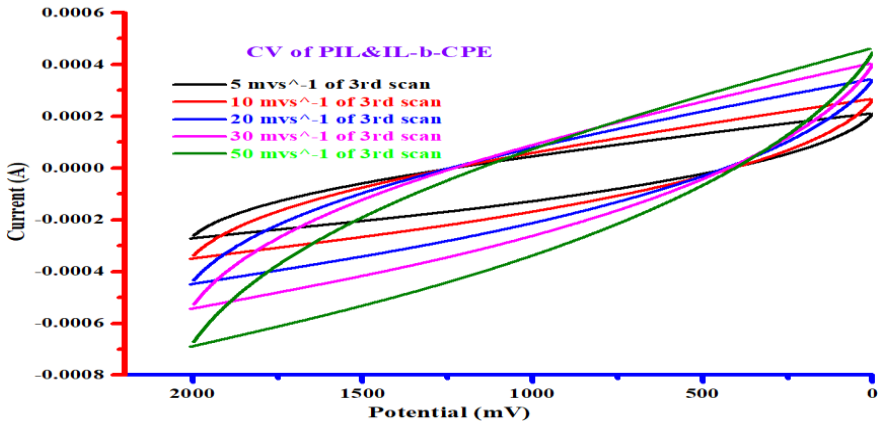

Figure 10 : CV curves of the ionic liquid based solid copolymer electrolyte supercapacitor measured at various bending states

The power delivered by the supercapacitor is given by the formula P = I* V, where I is the current and V is the voltage. In this case, the power is P = (-0.5 mA) * (2 V) = -1 mW. Since the power is negative, it indicates that the supercapacitor is discharging.

Energy Storage and Discharge: The energy stored in a supercapacitor is given by the formula E = (1/2) * C * V^2, where C is the capacitance. Given the voltage of 2 V and the current of -0.5 mA, we can calculate the capacitance using the formula I = C * (dV/dt). Solving for C, we find C = (2 * I) / (dV/ dt). Plugging in the values I = -0.5 mA and dV/dt = 2V/20 s (assuming a 20-second

charging scenario), we get ≈ 0.1 F. Now we can calculate the energy stored in the supercapacitor: E≈ (1/2) * 0.1 F* (2 V) ^2≈ 0.20 J. This energy will be dissipated during the discharge process.

Impact on Performance: The discharging of the supercapacitor will affect its performance in terms of the available power and the time it can supply the load. In this case, the supercapacitor can supply a load of -1 mW for a certain period, depending on the specific application and discharge voltage threshold.

Comparison with Other Energy Storage Devices: Comparing the energy storage and discharge characteristics of the supercapacitor with those of other energy storage devices, such as batteries, can provide insights into the relative performance of the two technologies for specific applications.

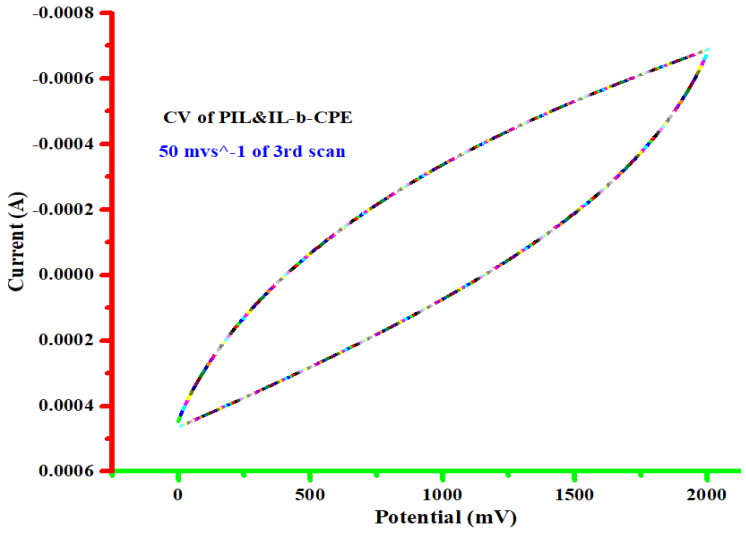

Figure 11 : Cyclic voltammograms of IL&PIL-b-CPE 04 of 50 mVS^-1

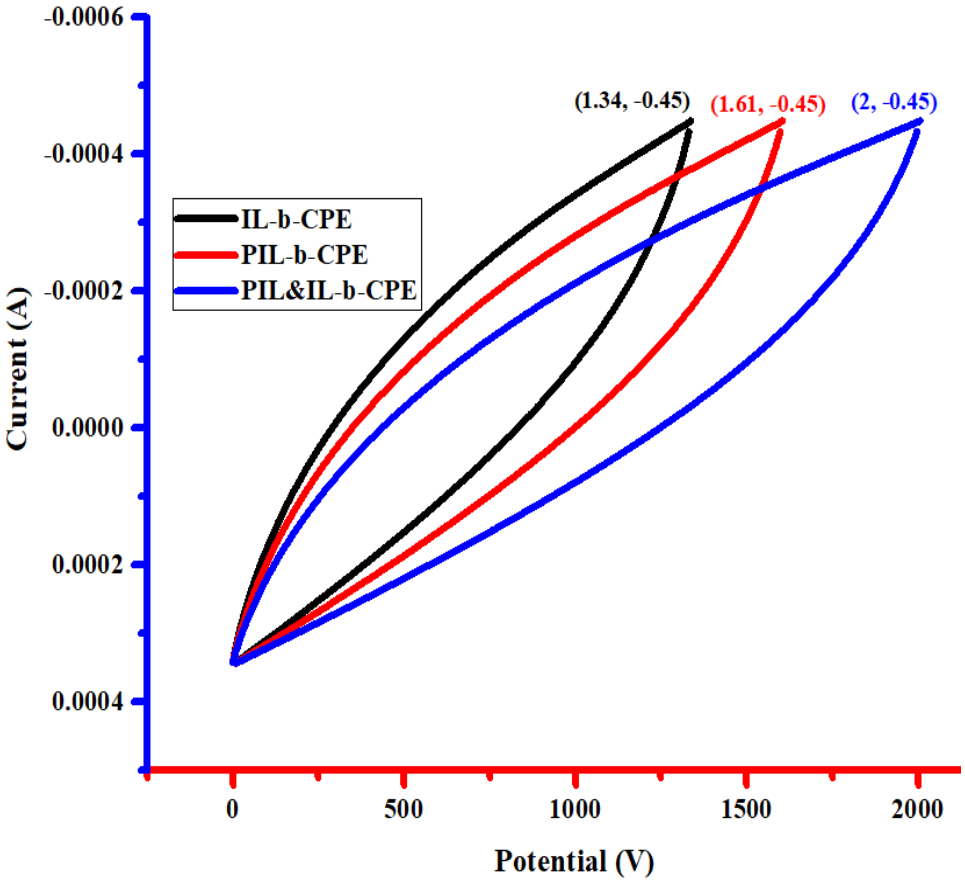

Figure 12 : CV graphs of IL-b-CPE, PIL-b-CPE and PIL&IL-b-CPE

As we can see in Figure 12 above, the graph of IL-b-CPE is 1.34 V, that of PIL-b-CPE is 1.61 V, and that of IL&PIL-b-CPE is 2 V. Based on this, we were able to see the difference in each of the solid polymer electrolyte capacitance in detail in Tables 2 and 3.

Energy Storage and Power Deliver the energy (E) stored in a supercapacitor is given by the formula E = (1/2) * C* V^2, where C is the capacitance and V is the voltage. We can calculate the voltage (V) using the given energy and capacitance values: V = sqrt (2* E/C)

For the given values of energy and capacitance:

V_1 = sqrt (2* 0.055 J / 0.065 F) ≈ 2.6 V

V_2 = sqrt (2* 0.102 J/ 0.08 F) ≈ 3.15 V

V_3 = sqrt (2* 0.2 J/0.1 F) ≈ 4.47 V

The power (P) delivered by the supercapacitor is given by the formula P = I * V, where I is the current. Given the negative power values, it indicates that negative power values, it means the supercapacitor is discharging. T_l. current (I) can be calculated as: I=P/V

For the given values of power and voltage:

I_1 = -0.65 mW/2.6 V~ -0.25 mA

1_2 = -0.8 mW/3.15 V~ -0.25 mA

1_3=-1 mW/4.47 V≈ -0.22 mA

Comparison of Capacitance and Energy: Supercapacitors with larger capacitance values can store more energy for a given voltage. The given values show that as the capacitance increases (0.065 F, 0.08 F, and 0.1 F), the energy also increases (0.055 J, 0.102 J, and 0.2 J). This indicates that a larger capacitance allows for greater energy

a) Impact on Performance: Supercapacitors with higher energy storage capacities can deliver power for a longer duration and support higher power applications. The given energy and power values indicate that the supercapacitors can supply power for different durations and loads, depending on their capacitance and voltage. Cyclic voltammetry (CV) tests of the SC were conducted at 5 - 50 mV S-1 in a two-electrode configuration to study the performance of the cell at different voltages, and in a three-electrode configuration in order to evaluate separately the electrochemical behavior of the positive and negative electrodes in the potential ranges determined by the galvanostatic experiments. The CV tests in the three-electrode configuration were performed using Pt wire as the counter electrode and an Ag wire as pseudo reference electrode. All of the electrochemical measurements were performed at 25 °C. The cell capacitance (Ccell), energy density (E), power density (P), and equivalent series resistance (ESR) were calculated from the galvanostatic curves and according to the cited reference (details of the calculations can be found in Supporting Information). Electrochemical behavior of all solid-state supercapacitors was determined by frequency response analysis. CD experiments will be conducted from 0 to 2 V at different current densities: 0.5, 0.4, 0.3, 0.2, and 0.1 mA cm^{-2}.

4.2.2. Electrochemical charge discharge

a) IL-b CPE

One of the most important ways to determine the electrochemical properties of a capacitor is to perform a charge-discharge test. Based on this, the charge and discharge rate of the impregnated carbon electrode obtained by adding IL at different ratios to CS/PAADDMAOH$^-$ was tested and it was reached to the 2 V set in the test standard.

Table 2 : Capacitance of IL-b-CPE

Electrode	Area	Active total mass (g)	Current density I(mA/cn^2)		slope Pte(mv/s)		Capacitance Ctam(F/g)	
	Cm^2	Gm	0.4mA	0.5mA	0.4mA	0.5mA	0.4mA	0.5mA
IL-b-CPE1	0.636	0.05	0.63	0.79	16.43	18.30	0.487	0.003
IL-b-CPE2	0.636	0.05	0.63	0.79	15.14	3.07	0.528	0.02
							Average =	**0.245**
								0.274

The impregnated solid-state copolymer electrolyte at a ratio of 1:0.25 showed the best results, and even when the charge level reached 2V voltage and 0.74 F/g capacitance, it was not possible to get that much stimulating capacitance. As a result, we have been needed to check at other options. This was illustrated in the following graph.

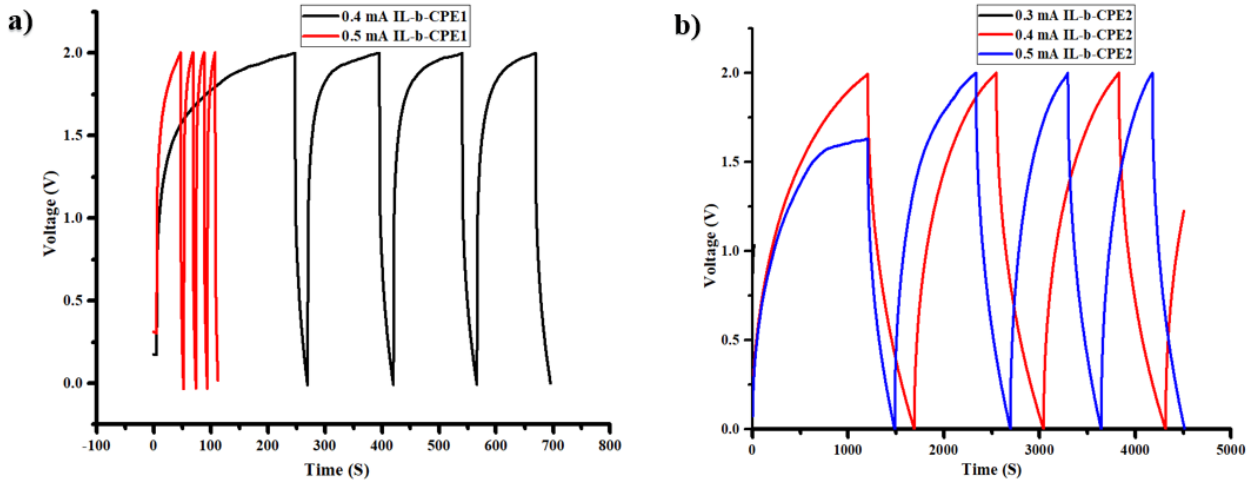

Figure 13 : a) Voltage Vs time graph on the ratio of 1:0.20. b) Voltage Vs time graph on the ratio of 1:0.25.

As we showed in Figure 13(a) above, there was no charge-discharge graph at 0.3 mA current density. Because the ionic liquid fills slowly with low current density when the amount of ionic liquid increases, it could not charge and discharge within the set time limit. This was further explained in Figure 14 by presented various studies as information. Similarly, in Figure 8(b), we can see a certain charge graph up to 1.0 V, but it cannot be discharged.

b) PIL-b-CPE

As a substitute of addition of pure PIL solution in to the CS-CPE mixture, different ratios of PIL were added into the mixtures of CS-CPE. Based on this, the charge and discharge rate of the impregnated carbon electrode attained by adding PIL at different ratios to IL-b-CPE was established and it was close to the 2 V set in the test parameter.

Table 3 : Capacitance of PIL-b-CPE

Electrode	**Area Cm^2**	**Am (g)**	**Current density I(mA/cm^2)**					**slope pte(mv/s)**					**Capacitance Ctam(F/g)**
			0.1 mA	**0.2 mA**	**0.3 mA**	**0.4 mA**	**0.5 mA**	**0.1 mA**	**0.2 mA**	**0.3 mA**	**0.4 mA**	**0.5 mA**	**0.1 mA - 0.5 mA**
PIL-b-CPE1	0.636	0.05	0.16	0.31	0.47	0.63	0.79	0.32	1.03	1.44	1.65	2.82	**1.391**
PIL-b-CPE2	0.636	0.05	0.16	0.31	0.47	0.63	0.79	0.33	0.38	0.43	0.51	0.61	**1.756**

The impregnated solid-state copolymer electrolyte at a ratio of 1:0.17 showed the best results, and even when the charge level reached 2V and 1.756 F/g capacitance, it was not possible to acquire that much encouraging capacitance. As a result, we wanted to look at other options. This was illustrated in figure 14.

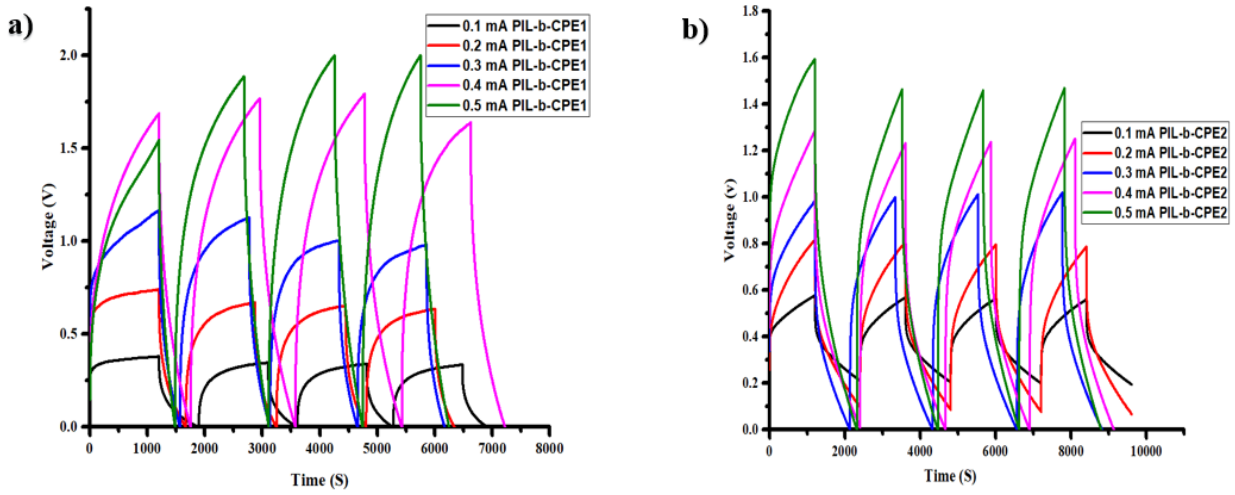

Figure 14 : a) Voltage Vs time graph on the ratio of 1:0.17. b) Voltage Vs time graph on the ratio of 1:0.20.

c) PIL&IL-bCPE

The solid copolymer electrolyte supercapacitor based on ionic liquid was subjected to a galvanostatic charge discharge (GCD) test at different current densities and room temperature. Charge discharge curves for various current densities at room temperature are displayed in Fig. 8. All of these profiles are almost symmetrical triangles with minimal voltage drop, even at high current densities, further confirming the supercapacitor's ideal capacitive behavior. For the actual application, it is imperative that the device's overall internal resistance be relatively minimal, as indicated by the slight voltage drop. The charge-discharge curves at various temperatures with a current density of 0.3 mA cm−2. At last addition of pure IL solution in to the PIL-b-CPE mixture, different ratios of IL were added into the mixtures of PIL-b-CPE. Based on this, the charge and discharge rate of the impregnated carbon electrode attained by adding PIL at different ratios to PIL&IL-b-CPE was established and it reached to the 2 V. The impregnated solid-state copolymer electrolyte at a ratio of 1:0.15 showed the best results. In addition to the fulfillment of the potential window that we set in the experimental parameter; the specific capacity energy density, power density and equivalent series resistance were able to show better results compared to what was done before and that we have seen above. This is more illustrated in the following section.

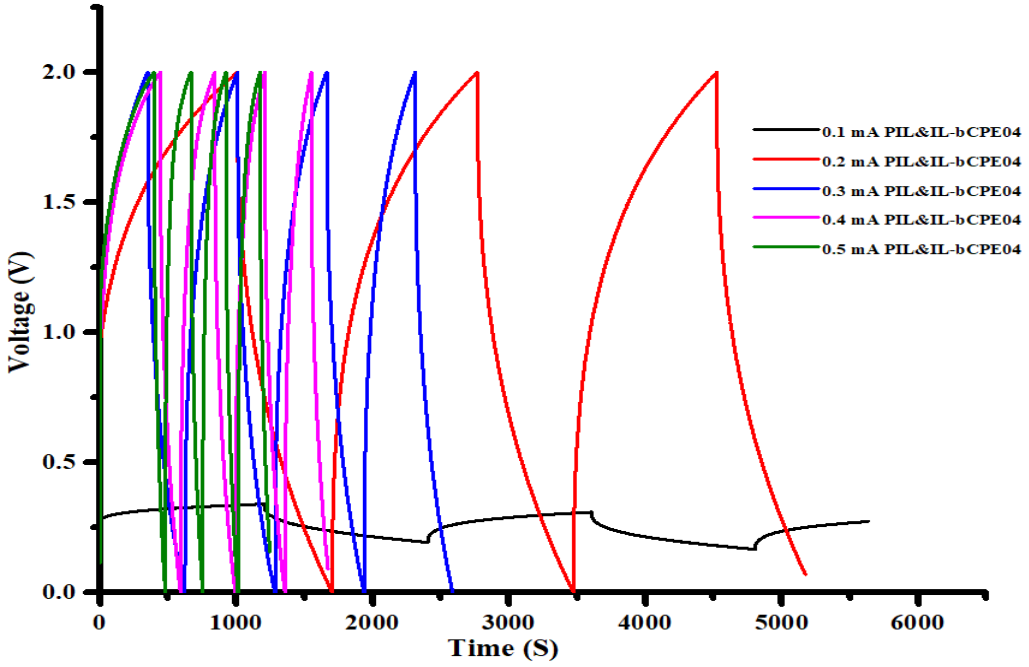

Figure 15 : Voltage Vs time graph on the ratio of PIL-b-CPE: IL = 1:0.15.

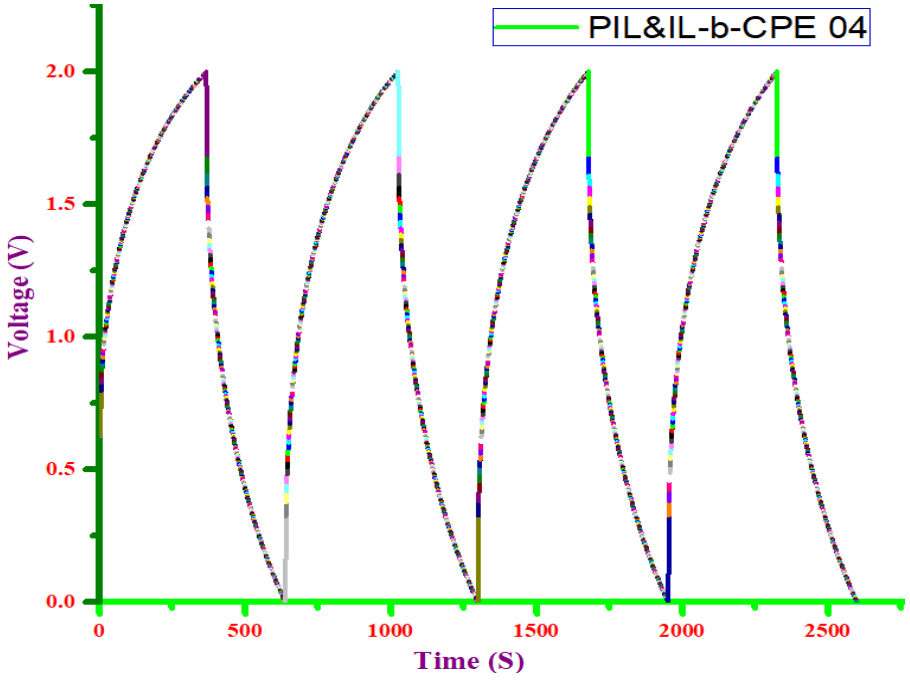

Figure 16 : Voltage Vs time graph on the ratio of PIL-b-CPE: IL = 1:0.15.

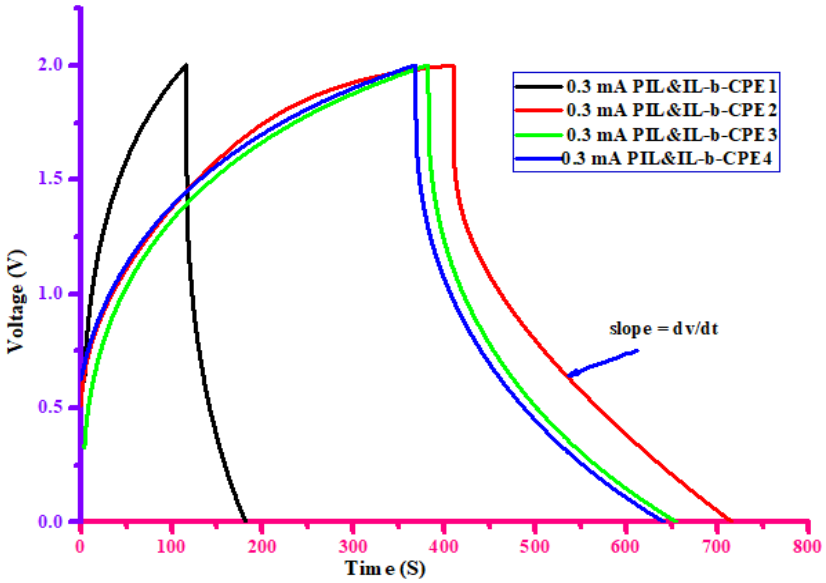

Figure 17 : Voltage Vs time graph on the ratio of PIL-b-CPE: IL = 1:0.15.

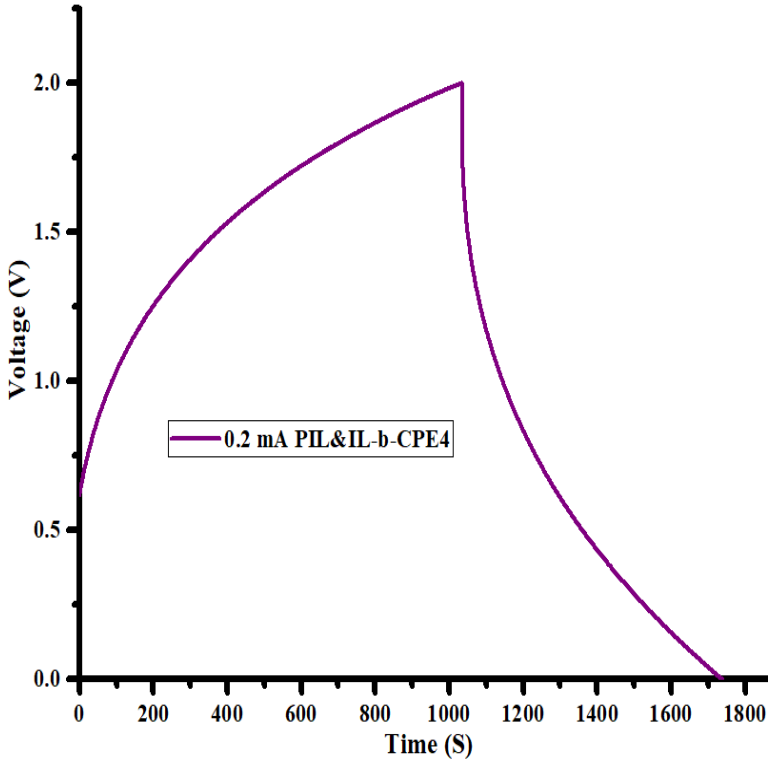

Figure 18 : Charge and Discharge of solid polymer electrolyte

The cell was in the discharged mode when it was assembled. After then, the cell was charged for 1030 (S) at a steady current of 0.2 mA, and a voltage of 2.0 V was reached. The solid copolymer

electrolyte (SCPE) was monitored for 1755 seconds at regular hourly intervals following discharging. The SPE of the cells decreased to 0 V, as shown by the graph in Figure 18.

Achieving the maximum operating voltage is essential to optimizing a SC's energy and power densities. Because the square of the voltage determines both cell characteristics, ILs electrolytes are strategically significant. Certain ILs are known to have incredibly huge stability windows. It is important to remember that the potentials supported at the electrolyte interface do not match the stability limits of the pure electrolyte, therefore this should not be interpreted as being similar to the operating voltage of the cells (80).

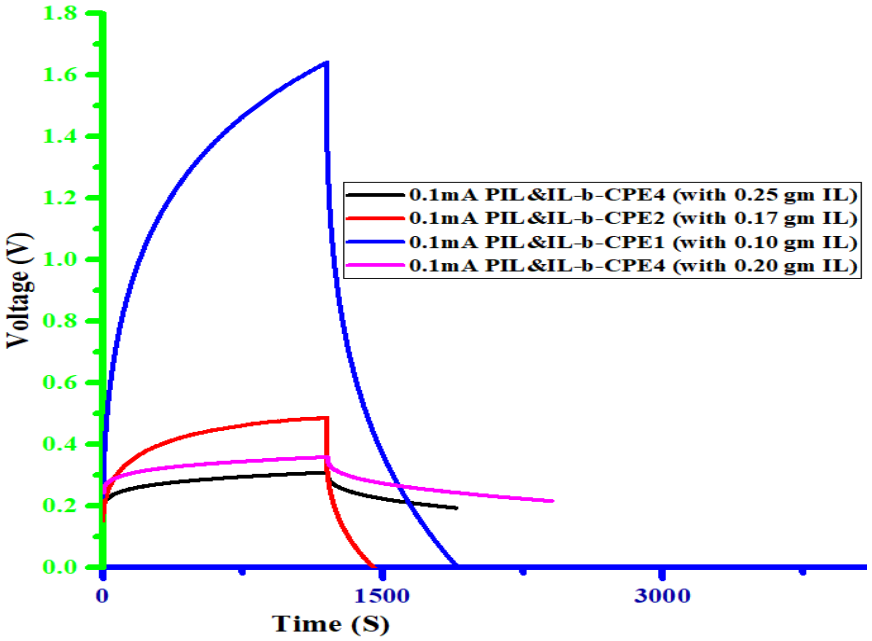

Figure 19 : Voltage Vs time graph of 0.1 mA PIL&IL-b-CPE with different ratio of ionic liquid

As a result, ILs exhibit higher resistance to ionic diffusion than other electrolytes, as well as superior resistance at the interface, where ions attempt to enters the porous network of the electrodes. Moreover, at high voltages, the high resistances that impact cell efficiency worsen. (77). As the concentration of the ionic liquid increases, the viscosity of the electrolyte increases. This makes it difficult to increase the potential difference using the low current density. Accordingly, as the percentage of ionic liquid increases, the voltage decreases.

The specific capacitances of the solid-state copolymer electrolyte supercapacitor at ambient temperature are calculated by eqn (1) from their relevant discharge curve at different current densities and are presented in Fig. 13. The specific capacitances (Cs) are 1.22 F g^{-1}, 3.08 F g^{-1},

3.65 F g^{-1} and 3.71 F g^{-1} at 10 %, 17 %, 20 %, 25 % of ionic liquid (discharge current density is 0.3 – 0.8 mA cm^{-2}), respectively. It is noticed that the specific capacitances increase with the ionic liquid increase, the reason is the higher ionic conductivity of the polymer electrolyte at high ionic liquid, and the high ionic conductivity promoting the amount of ions diffuse into electric double layer electrode (81). With the increasing discharge current density, the specific capacitances decrease slightly, and this trend is fit in to many previously articles about supercapacitor (82,83).

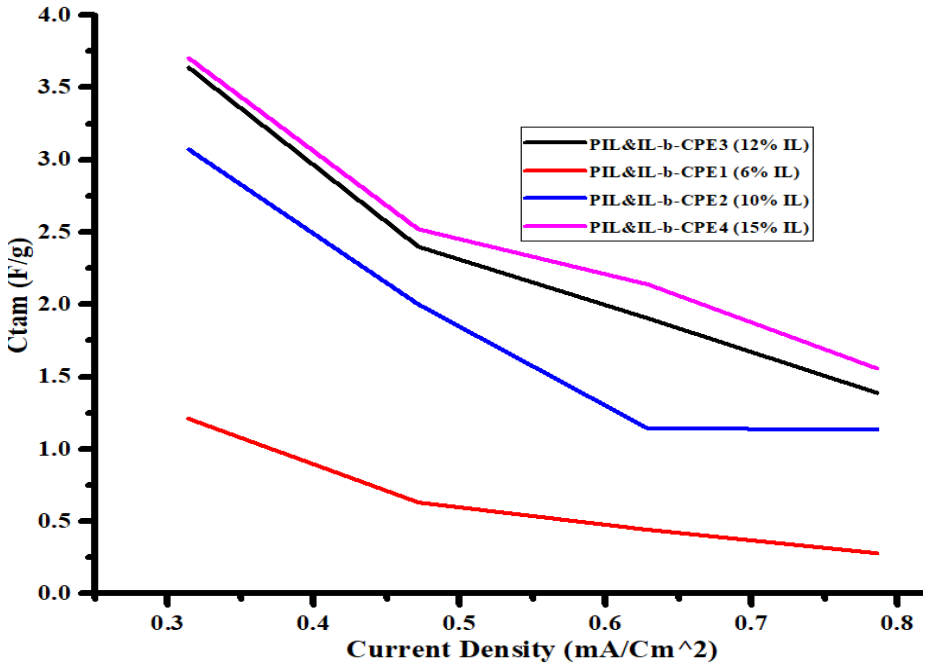

Figure 20 : Capacitance Vs Current density graph

Typical Capacitance Current density characteristic curves of the fabricated cell are as shown in Fig. 20. During charging at 25 % of Ionic liquid (IL) for 0.3 mA/cm^2, the cell acquired a Capacitance is 3.74 F/g. Upon Capacitance at 10 % of Ionic liquid (IL), the Capacitance dropped to 1.23 F/g. Since at the end of the charging capacity of the cell is 25 % PIL&IL-b-CPE4.

Characterization of Electrochemical Capacitors via Electrochemistry The performance of each electrode material in an EC can be evaluated using a variety of instruments.

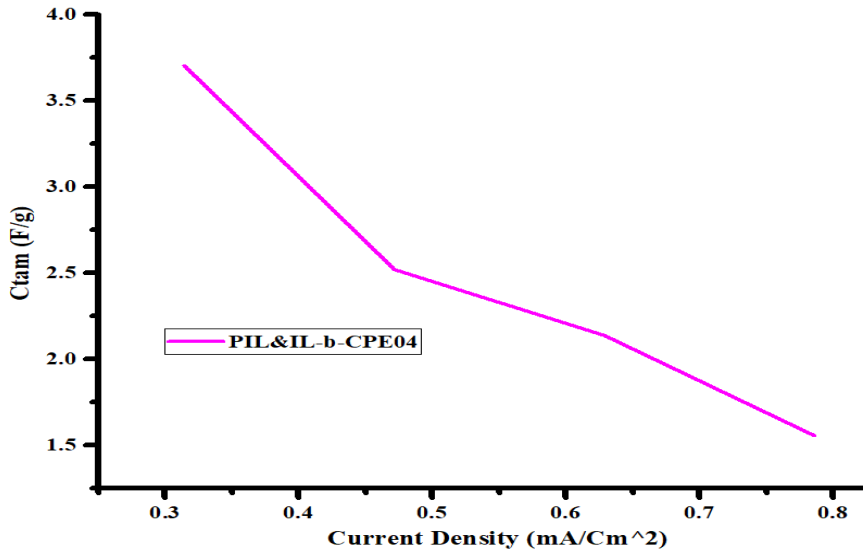

Figure 21 : specific capacitance of a single electrode

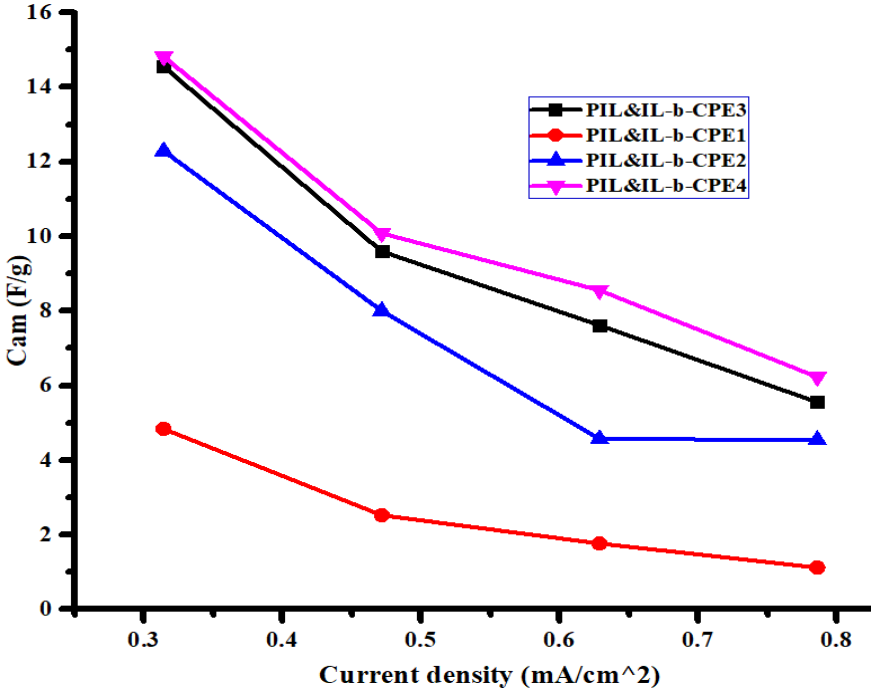

Figure 22 : the capacitance of the two-electrode

In this case, the value that will be estimated for the capacitor (Ctot) will be smaller than that found for the single electrode and given by

$$\frac{1}{C_{tot}} = \frac{1}{C_+} + \frac{1}{C_-} \qquad (4.4)$$

Where, the capacitance of the positive and negative electrodes is denoted by C+ and C-, respectively. Now, it's critical to discuss a subject that occasionally causes confusion in the literature: the difference of a factor of four between the capacitance of a single electrode and a symmetric two-electrode EC. According to (4.4), the gravimetric capacitance of the capacitor will become Ctot/2, giving this factor of 4, if the capacitance (C+ and C-) and the weight (m) of both electrodes are the same (i.e., a total weight of 2m). Later on, this matter will also be covered. The constant current charge/discharge cycles of a two-electrode capacitor can be used to calculate the real power density Preal (W/kg) and the real energy Ereal (Wh/kg).

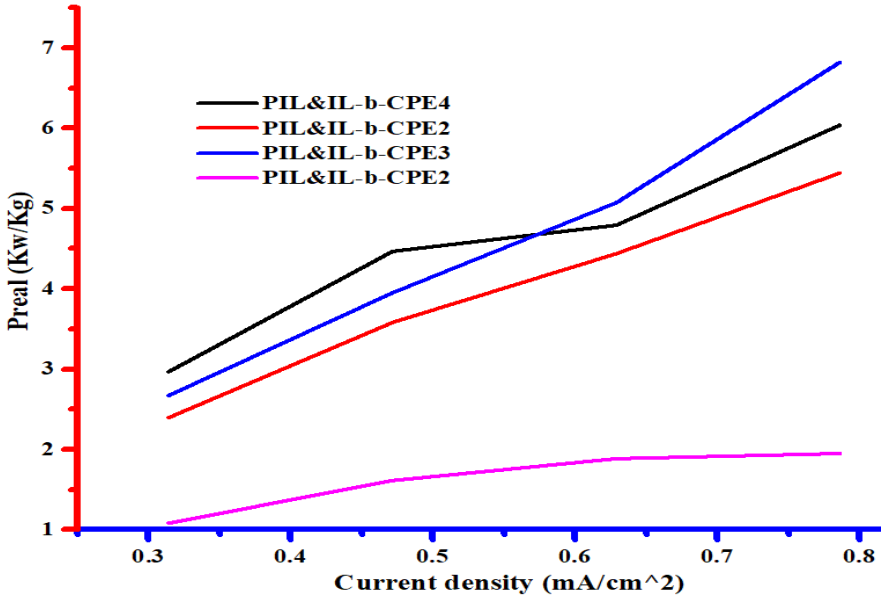

Figure 23 : graph of the real power density Preal

$$P_{real} = \frac{\Delta EI}{m} \qquad (3)$$

Where ΔE = (Emax + Emin/2) with Emax is the potential at the end of charge and E min at the end of discharge, I the applied current, and m the weight of active material of the electrodes

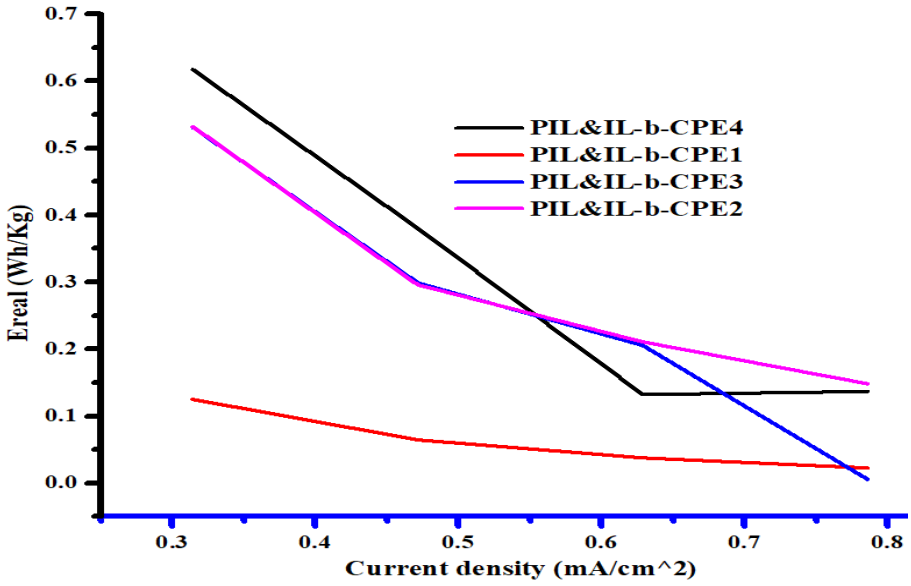

Figure 24 : the real energy density Ereal

$$E_{real} = p_{real}t \qquad (4)$$

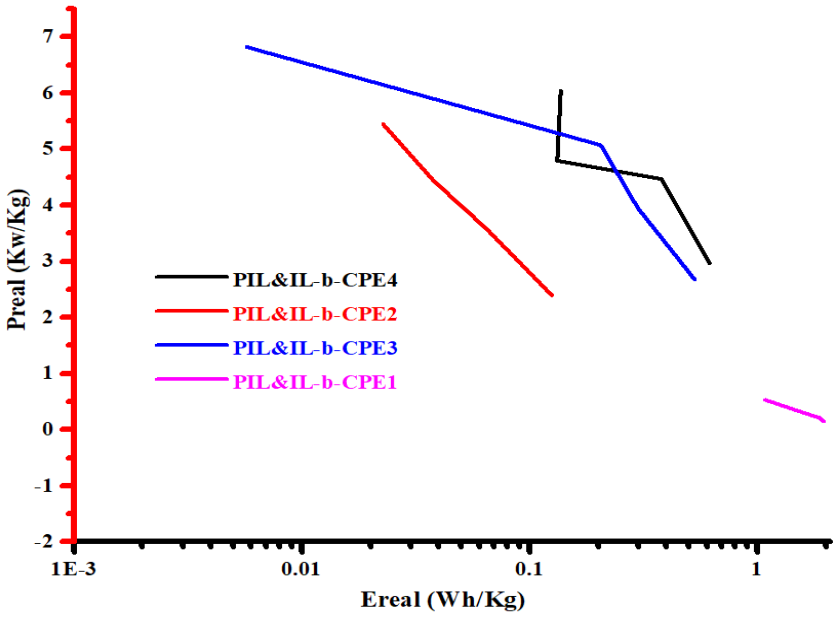

Figure 25 : graph of the real Energy density (Ereal) graph

Energy density (E, Wh kg^{-1}) and power density (P, W kg^{-1}) are also two essential factors for weighing the electrochemical behavior. Which were deliberate according to eqn. (3) and (4). Fig. 25 shows the energy density Emax. (Wh kg^{-1}) and power density (P, W kg^{-1}) of the supercapacitor at different temperature with different current densities. It is obvious that the supercapacitor at

25% ionic liquid shows the highest energy density of 2.08 Wh kg^{-1} and the power density of 4.5 kW kg^{-1} at 0.3 mA cm^{-2}, and remains the 0.86 Wh kg^{-1} and 15 W kg^{-1} at 0.8 mA cm^{-2}. The comparison of energy density and power density of supercapacitor at 10% ionic liquid is only 0.68 Wh kg^{-1} and 10 W kg^{-1} at 0.3 mA cm^{-2}, and energy density of supercapacitor at 25% ionic liquid was significantly increased by 306% compared to the supercapacitor. The greater ionic conductivity of the ionic liquid-based polymer electrolyte at high ionic liquid percentage is responsible for the better electrochemical performances of the supercapacitor at 10% ionic liquid. These results are consistent with the specific capacitances of supercapacitors. To provide a more thorough comparison with the performance of ionic liquid-based solid-state copolymer electrolyte supercapacitors, Table 4 presents a range of supercapacitor data from prior papers.

Table 4 : Performance comparison of Ionic liquid based solid polymer electrolyte supercapacitor with different polymer electrolytes from previous literature

Electrodes materials	Polymer electrolytes	Cs (F g^{-1})	Ereal (Wh kg^{-1})	Voltage (V)	Reference
CNT-graphite	CS-PAADDA-OH-	2.73 (RT)	--	1.2	(15)
AC	PAEK-PEG/$LiClO_4$	103.17 (120 ^oC)	6.76 (120 ^oC)	1.5	(81)
AC	PAES-Q-1.1[b]	92.79 (RT)	2.61 (RT)	1	(84)
AC	PEO/6 M KOH	90 (RT)	--	1	(85)
AC[a]	PIL&IL-b-CPE04	3.74 (RT)	2.07 (RT)	2	This work

Alternatively, the maximum specific power, Pmax, can be calculated from

$$P_{max} = \frac{U_0^2}{4Rm} \text{ (W/kg)} \qquad (4.5)$$

Where U_0 is the potential at the beginning of discharge (after the ohmic drop) and R the internal resistance measured.

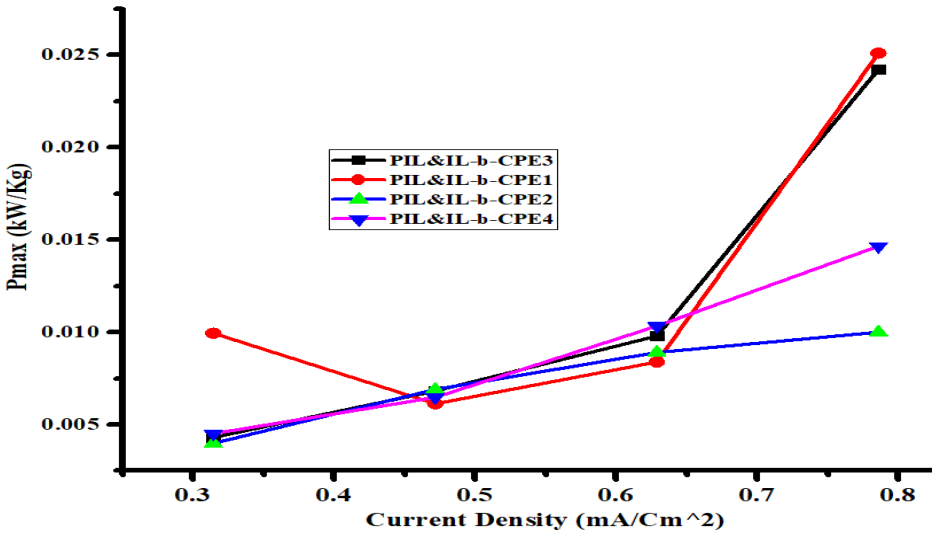

Figure 26 : graph of the maximum specific power (Pmax)

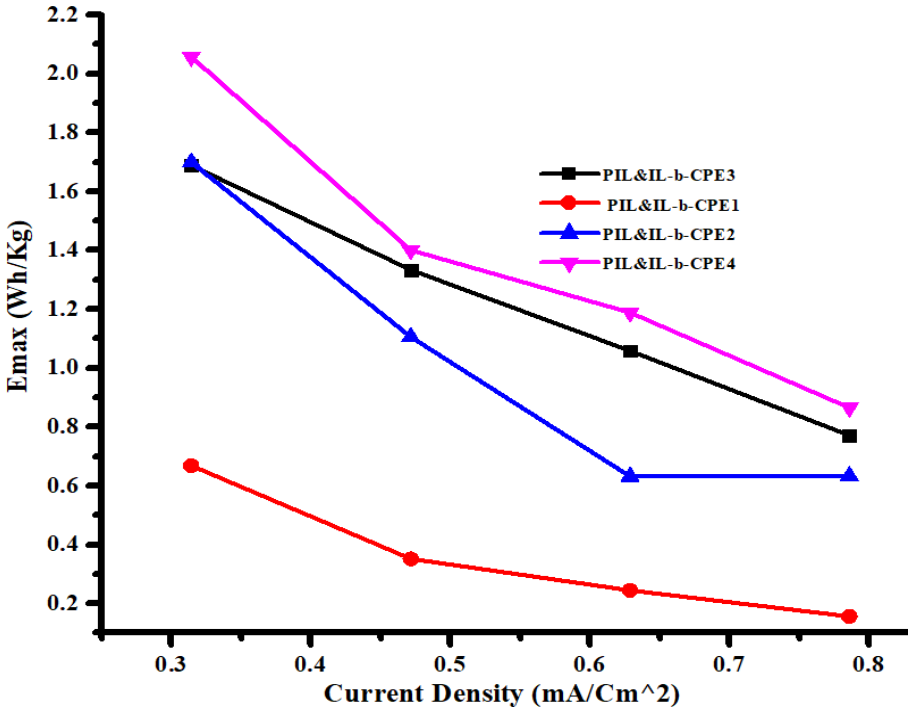

Figure 27 : graph of the maximum stored specific energy (Emax)

The maximum stored specific energy is defined as

$$E_{max} = \frac{C(U_{max})^2}{2} \quad \text{(Wh/kg)} \qquad (4.6)$$

Where C is the system capacity and U_{max} the potential at the end of discharge.

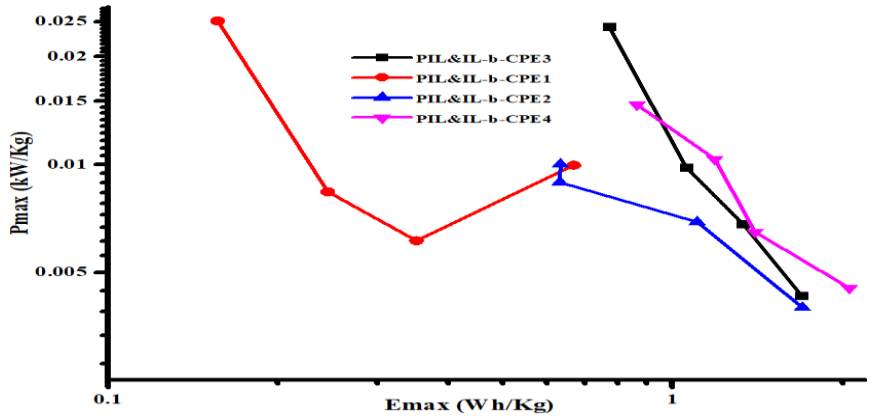

Figure 28 : Emax Vs Pmax graph

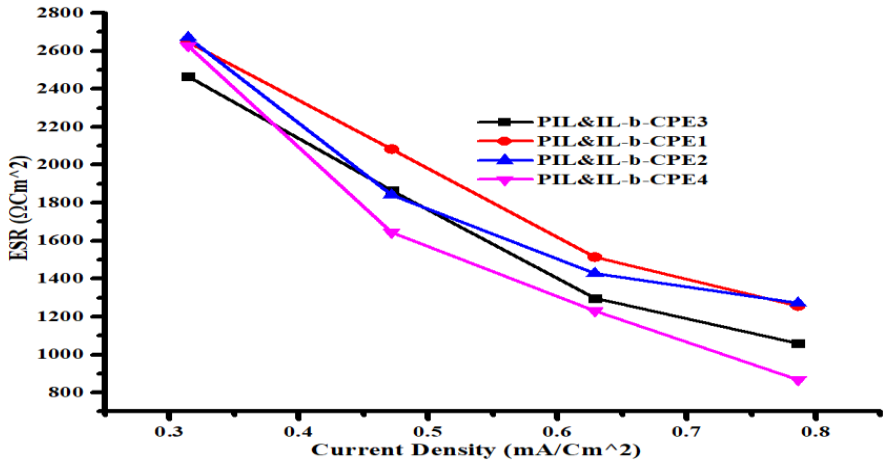

Figure 29 : The equivalent series resistance (ESR) graph

The equivalent series resistance (ESR) and columbic efficiency are two more helpful characteristics that describe an EC. The ratio of charge to discharge time yields the columbic efficiency. When the columbic efficiency is 1, there are no side reactions during the charge or discharge phases. On the other hand, the current interrupt approach at both ends of charge can be used to measure the ESR.

CHAPTER FIVE

5. CONCLUSION AND RECOMMENDATIONS

5.1. CONCLUSION

This work presents the effective organization of a series of innovative PIL&IL-b-CPE polymer electrolyte membranes by a combination technique, followed by their application in a solid electrochemical capacitor system. When the PAADDA mass fraction was 33%, the polymer electrolyte membrane showed a compact interpenetrating polymer network structure with a moderately high capacitance (3.74 F/g) at room temperature. Furthermore, the membrane demonstrated robust mechanical and alkaline stability, along with a comparatively elevated oxidative durability, under exposure to a 50 milliliter H2O solution at room temperature. The coupled cross-linking that improved the membranes' stability may be the cause of the aforementioned findings. This alkaline polymer electrolyte membrane demonstrated a broad potential window (2 V) in a solid symmetric activated carbon cell with respect to electrochemical characterizations. Furthermore, the membrane exhibited strong stability during 1700 cycles of charging and discharging. These results imply that an appealing electrolyte for the solid electrochemical capacitors is the PIL&IL-b-CPE polymer membrane. In addition to the quick development of new technologies for energy storage. It has been shown that by eliminating the interfaces that limit capacitance and by using a new voltage to establish the stability limits of an electrolyte, this novel concept enables surpassing the energy density of traditional cells. Furthermore, it has been demonstrated that ionic-based solid copolymer electrolyte SCs are extremely versatile since they may be configured in a symmetric, lopsided, or fusion manner to maximize their electrochemical performance without requiring additional technological complexity during cell building. The combination of PIL and IL-b-CPE resulted in the largest cell capacitance and maximum voltage, with an energy density of 2.07 W h kg^-1. Furthermore, this perspective might serve as a foundation for researchers in this area to enhance novel devices with further asymmetries including various electrodes, electrolytes, and storage methods in order to attain long-term performance and high energy and power densities.

5.2. Recommendations

The following issues are suggested to be investigated further: Another crucial limitation for any solid-state supercapacitor is strength performance. It is advised to conduct pedestrian galvanostatic charge-discharge tests at various cycles and temperatures in order to evaluate the practical uses of the supercapacitor at high temperatures. This is necessary in order to obtain the cycle life test of the as-fabricate supercapacitor.

We suggest expanding the range of applications for this synthetic polymer membrane to include alkaline batteries, nickel metal hydride batteries, and alkaline fuel cells.

In order to make the results of the experimental test more reliable and to find out important electronic and charge instructions that were not seen during the experimental test, we recommend that the work done be done by a computational method.

5.3. References

1. Lewandowski A, Olejniczak A, Galinski M, Stepniak I. Performance of carbon-carbon supercapacitors based on organic, aqueous and ionic liquid electrolytes. J Power Sources 2010;195(17):5814–9.
2. Gallagher TM, Ciocanel C, Browder C. Structural load bearing supercapacitors using a pegdge based solid polymer electrolyte matrix. ASME 2011 Conf Smart Mater Adapt Struct Intell Syst SMASIS 2011. 2011;1:141–8.
3. Frackowiak E, Khomenko V, Jurewicz K, Lota K, Béguin F. Supercapacitors based on conducting polymers/nanotubes composites. J Power Sources. 2006;153(2):413–8.
4. Ellenbogen JC. Supercapacitors : A Brief Overview. 2006;(March).
5. Wang G, Wang H, Zhong B, Zhang L, Zhang J. Supercapacitors' Applications. 2015;(April 2018):479–92.
6. Tiruye GA, Muñoz-Torrero D, Palma J, Anderson M, Marcilla R. Performance of solid state supercapacitors based on polymer electrolytes containing different ionic liquids. J Power Sources. 2016;326:560–8.
7. Minakshi Sundaram M, Mitchell ,2017;46(40):13704–13.
8. Banerjee S, De B, Sinha P, Cherusseri J, Kar KK. Applications of supercapacitors. Vol. 300, Springer Series in Materials Science. 2020. 341–350 p.
9. Wang P, Zakeeruddin SM, Moser JE, Grätzel M. A new ionic liquid electrolyte enhances the conversion efficiency of dye-sensitized solar cells. J Phys Chem B. 2003;107(48):13280–5.
10. Ito S, Tanaka S, Nishino H. Lead-halide perovskite solar cells by CH3NH3I dripping on PbI2-CH3NH3I-DMSO precursor layer for planar and porous structures using CuSCN hole-transporting material. J Phys Chem Lett. 2015;6(5):881–6.
11. Cui M, Meng X. Overview of transition metal-based composite materials for supercapacitor electrodes. Nanoscale Adv. 2020;2(12):5516–28.
12. Poonam, Sharma K, Arora A, Tripathi SK. Review of supercapacitors: Materials and devices. J Energy Storage. 2019;21(October 2018):801–25.

13. Manuel Stephan A, Nahm KS. Review on composite polymer electrolytes for lithium batteries. Polymer (Guildf). 2006;47(16):5952–64.

14. Yang Z, Peng H, Wang W, Liu T. Crystallization behavior of poly(ε-caprolactone)/layered double hydroxide nanocomposites. J Appl Polym Sci. 2010;116(5):2658–67.

15. Ao B, Wei Y, Wang M, Et al, 2018.04.133

16. Srivastava N, Tiwari T. New trends in polymer electrolytes: A review. E-Polymers. 2009;(146):1–17.

17. Zhao Y, Wu C, 2016;301(July):47–53. Available from:

18. Albinsson I, Mellander BE, Stevens JR. Ion association effects and ionic conductivity in polymer electrolytes. Solid State Ionics. 1993;60(1–3):63–6.

19. Ngai KS, Ramesh S, 2016;22(8):1259–79. Available from:

20. Fenton DE, Parker JM, Wright P V. Complexes of alkali metal ions with poly(ethylene oxide). Polymer (Guildf). 1973;14(11):589.

21. Li J, Qiao J, Lian K. Hydroxide ion conducting polymer electrolytes and their applications in solid supercapacitors: A review. Energy Storage Mater. 2020;24:6–21. Available from:

22. Li J, Qiao J, Lian K. Investigation of polyacrylamide based hydroxide ion-conducting electrolyte and its application in all-solid electrochemical capacitors. Sustain Energy Fuels. 2017;1(7):1580–7.

23. Gao H, Li J, Miller JR, Outlaw RA, Butler S, Lian K. Solid-state electric double layer capacitors for ac line-filtering. Energy Storage Mater [Internet]. 2016;4:66–70.

24. Lee KH, Lee YG, Park JK, Seung DY. Effect of silica on the electrochemical characteristics of the plasticized polymer electrolytes based on the P(AN-co-MMA) copolymer. Solid State Ionics. 2000;133(3):257–63.

25. Shieh JJ, Huang RYM. Pervaporation with chitosan membranes II. Blend membranes of chitosan and polyacrylic acid and comparison of homogeneous and composite membrane based on polyelectrolyte complexes of chitosan and polyacrylic acid for the separation of ethanol-water mixture. J Memb Sci. 1997;127(2):185–202.

26. Ramkumar R, Minakshi M. Fabrication of ultrathin CoMoO4 nanosheets modified with

chitosan and their improved performance in energy storage device. Dalt Trans. 2015;44(13):6158–68.

27. Ramkumar R, Minakshi Sundaram M. A biopolymer gel-decorated cobalt molybdate nanowafer: Effective graft polymer cross-linked with an organic acid for better energy storage. New J Chem [Internet]. 2016;40(3):2863–77.

28. Biswal A, Minakshi M, Tripathy BC. Probing the electrochemical properties of biopolymer modified EMD nanoflakes through electrodeposition for high performance alkaline batteries. Dalt Trans. 2016;45(13):5557–67.

29. Li X, Liu L, Wang X, Ok YS, Elliott JAW, Chang SX, et al. Flexible and Self-Healing Aqueous Supercapacitors for Low Temperature Applications: Polyampholyte Gel Electrolytes with Biochar Electrodes. Sci Rep [Internet]. 2017;7(1):1–11.

30. Qiao YQ, Wang XL, Xiang JY, Zhang D, Liu WL, Tu JP. Electrochemical performance of Li3V2(PO 4)3/C cathode materials using stearic acid as a carbon source. Electrochim Acta. 2011;56(5):2269–75.

31. Latip NAA, Ng HM, Farah N, Ramesh K, Ramesh S, Ramesh S. Novel development towards preparation of highly efficient ionic liquid based co-polymer electrolytes and its application in dye-sensitized solar cells. Org Electron. 2017;41:33–41.

32. Ayalneh Tiruye G, Muñoz-Torrero D, Palma J, Anderson M, Marcilla R. All-solid state supercapacitors operating at 3.5 v by using ionic liquid based polymer electrolytes. J Power Sources. 2015;279:472–80.

33. Kandalkar SG, Dhawale DS, Kim CK, Lokhande CD. Chemical synthesis of cobalt oxide thin film electrode for supercapacitor application. Synth Met [Internet]. 2010;160(11–12):1299–302.

34. Smyth R. Are fluctuations in energy variables permanent or transitory? A survey of the literature on the integration properties of energy consumption and production. Appl Energy [Internet]. 2013;104:371–8.

35. Winter M, Brodd RJ. What are batteries, fuel cells, and supercapacitors? Chem Rev. 2004;104(10):4245–69.

36. Yang Z, Tian J, Ye Z, Jin Y, Cui C, Xie Q, et al. High energy and high power density

supercapacitor with 3D Al foam-based thick graphene electrode: Fabrication and simulation. Energy Storage Mater [Internet]. 2020;33:18–25.

37. Nanocrystal PS. PANI-Sol nanocrystal. J Energy Storage [Internet]. 2020;31(April):101652.

38. Lu X, Yu M, Wang G, Tong Y, Li Y. Flexible solid-state supercapacitors: Design, fabrication and applications. Energy Environ Sci. 2014;7(7):2160–81.

39. Kandambeth S, Jia J, Wu H, Kale VS, Parvatkar PT, Czaban-Jóźwiak J, et al. Covalent Organic Frameworks as Negative Electrodes for High-Performance Asymmetric Supercapacitors. Adv Energy Mater. 2020;10(38):1–9.

40. Sajjad M, Lu W. Covalent organic frameworks based nanomaterials: Design, synthesis, and current status for supercapacitor applications: A review. J Energy Storage [Internet]. 2021;39(April):102618.

41. Wang KB, Xun Q, Zhang Q. Recent progress in metal-organic frameworks as active materials for supercapacitors. EnergyChem [Internet]. 2020;2(1):100025.

42. Boorboor Ajdari F, Kowsari E, Niknam Shahrak M, Ehsani A, Kiaei Z, Torkzaban H, et al. A review on the field patents and recent developments over the application of metal organic frameworks (MOFs) in supercapacitors. Coord Chem Rev [Internet]. 2020;422:213441.

43. Fattah NFA, Ng HM, Mahipal YK, Numan A, Ramesh S, Ramesh K. An approach to solid-state electrical double layer capacitors fabricated with graphene oxide-doped, ionic liquid-based solid copolymer electrolytes. Materials (Basel). 2016;9(6).

44. Huang J, Sumpter BG, Meunier V. A universal model for nanoporous carbon supercapacitors applicable to diverse pore regimes, carbon materials, and electrolytes. Chem - A Eur J. 2008;14(22):6614–26.

45. Muzaffar A, Ahamed MB, Deshmukh K, Thirumalai J. A review on recent advances in hybrid supercapacitors: Design, fabrication and applications. Renew Sustain Energy Rev. 2019;101(October 2018):123–45.

46. Noori A, El-Kady MF, Rahmanifar MS, Kaner RB, Mousavi MF. Towards establishing standard performance metrics for batteries, supercapacitors and beyond. Chem Soc Rev.

2019;48(5):1272–341.

47. Hallinan DT, Balsara NP. Polymer electrolytes. Annu Rev Mater Res. 2013;43:503–25.

48. Wright P V. Developments in polymer electrolytes for lithium batteries. MRS Bull. 2002;27(8):597–602.

49. Manuel Stephan A. Nanocomposite polymer electrolytes for lithium batteries. Recent Adv Polym Nanocomposites. 2009;394(July):455–82.

50. Wang L, Li X, Yang W. Enhancement of electrochemical properties of hot-pressed poly(ethylene oxide)-based nanocomposite polymer electrolyte films for all-solid-state lithium polymer batteries. Electrochim Acta [Internet]. 2010;55(6):1895–9.

51. Wang YU. Gum-like nanocomposites as interfacial energy materials for energy storage devices. 2015;(August).

52. Vakhshouri K, Smith BH, Chan EP, Wang C, Salleo A, Wang C, et al. Signatures of intracrystallite and intercrystallite limitations of charge transport in polythiophenes. Macromolecules. 2016;49(19):7359–69.

53. Agapov AL, Sokolov AP. Decoupling ionic conductivity from structural relaxation: A way to solid polymer electrolytes? Macromolecules. 2011;44(11):4410–4.

54. Borodin O, Smith GD. Mechanism of ion transport in amorphous poly(ethylene oxide)/ LiTFSI from molecular dynamics simulations. Macromolecules. 2006;39(4):1620–9.

55. Chintapalli S, Frech R. Effect of plasticizers on ionic association and conductivity in the (PEO)9LiCF3SO3 system. Macromolecules. 1996;29(10):3499–506.

56. Teran AA, Tang MH, Mullin SA, Balsara NP. Effect of molecular weight on conductivity of polymer electrolytes. Solid State Ionics [Internet]. 2011;203(1):18–21.

57. Endo K, Matsuda Y. Study of a new polymer electrolyte poly(ethylene oxide): NaClO3 with several plasticizers for battery application. Polym Int. 2001;50(1):89–94.

58. Huq R, Koksbang R, Tonder PE, Farrington GC. Effect of plasticizers on the properties of new ambient temperature polymer electrolyte. Electrochim Acta. 1992;37(9):1681–4.

59. Gadjourova Z, Andreev YG, Tunstall DP, Bruce PG. Ionic conductivity in crystalline polymer electrolytes. Nature. 2001;412(6846):520–3.

60. Dissanayake MAKL, Jayathilaka PARD, Bokalawala RSP, Albinsson I, Mellander BE. Effect of concentration and grain size of alumina filler on the ionic conductivity enhancement of the (PEO)9LiCF3SO3:Al2O3 composite polymer electrolyte. J Power Sources. 2003;119–121:409–14.

61. Tang C, Hackenberg K, Fu Q, Ajayan PM, Ardebili H. High ion conducting polymer nanocomposite electrolytes using hybrid nanofillers. Nano Lett. 2012;12(3):1152–6.

62. Adebahr J, Byrne N, Forsyth M, MacFarlane DR, Jacobsson P. Enhancement of ion dynamics in PMMA-based gels with addition of TiO2 nano-particles. Electrochim Acta. 2003;48(14-16 SPEC.):2099–103.

63. Wang XL, Mei A, Li M, Lin YH, Nan CW. Polymer composite electrolytes containing ionically active mesoporous SiO2 particles. J Appl Phys. 2007;102(5):5–11.

64. Young WS, Epps TH. Ionic conductivities of block copolymer electrolytes with various conducting pathways: Sample preparation and processing considerations. Macromolecules. 2012;45(11):4689–97.

65. Wang Y, Zhong WH. Development of electrolytes towards achieving safe and high-performance energy-storage devices: A review. ChemElectroChem. 2015;2(1):22–36.

66. Giles JRM, Gray FM, MacCallum JR, Vincent CA. Synthesis and characterization of ABA block copolymer-based polymer electrolytes. Polymer (Guildf). 1987;28(11):1977–81.

67. Gray FM, MacCallum JR, Vincent CA, Giles JRM. Novel Polymer Electrolytes Based on ABA Block Copolymers. Macromolecules. 1988;21(2):392–7.

68. Panday A, Mullin S, Gomez ED, Wanakule N, Chen VL, Hexemer A, et al. Effect of molecular weight and salt concentration on conductivity of block copolymer electrolytes. Macromolecules. 2009;42(13):4632–7.

69. Wang C, Sakai T, Watanabe O, Hirahara K, Nakanishi T. All Solid-State Lithium-Polymer Battery Using a Self-Cross-Linking Polymer Electrolyte. J Electrochem Soc. 2003;150(9):A1166.

70. Hallinan DT, Mullin SA, Stone GM, Balsara NP. Lithium Metal Stability in Batteries with Block Copolymer Electrolytes. J Electrochem Soc. 2013;160(3):A464–70.

71. Park MJ, Choi I, Hong J, Kim O. Polymer electrolytes integrated with ionic liquids for future electrochemical devices. J Appl Polym Sci. 2013;129(5):2363–76.

72. Young WS, Kuan WF, Epps TH. Block copolymer electrolytes for rechargeable lithium batteries. J Polym Sci Part B Polym Phys. 2014;52(1):1–16.

73. Mullin SA, Stone GM, Panday A, Balsara NP. Salt Diffusion Coefficients in Block Copolymer Electrolytes. J Electrochem Soc. 2011;158(6):A619.

74. Weber RL, Ye Y, Schmitt AL, Banik SM, Elabd YA, Mahanthappa MK. Effect of nanoscale morphology on the conductivity of polymerized ionic liquid block copolymers. Macromolecules. 2011;44(14):5727–35.

75. Mullin SA, Teran AA, Yuan R, Balsara NP. Effect of thermal history on the ionic conductivity of block copolymer electrolytes. J Polym Sci Part B Polym Phys. 2013;51(12):927–34.

76. Sagadevan S, Marlinda AR, Chowdhury ZZ, Wahab YBA, Hamizi NA, Shahid MM, et al. Fundamental electrochemical energy storage systems [Internet]. Advances in Supercapacitor and Supercapattery: Innovations in Energy Storage Devices. INC; 2020. 27–43 p.

77. Santos MCG, Silva GG, Santamariá R, Ortega PFR, Lavall RL. Discussion on operational voltage and efficiencies of ionic-liquid-based electrochemical capacitors. J Phys Chem C. 2019;123(14):8541–9.

78. Qiao J, Hamaya T, Okada T. New highly proton-conducting membrane poly(vinylpyrrolidone)(PVP) modified poly(vinyl alcohol)/2-acrylamido-2-methyl-1-propanesulfonic acid (PVA-PAMPS) for low temperature direct methanol fuel cells (DMFCs). Polymer (Guildf). 2005;46(24):10809–16.

79. Qiao J, Fu J, Liu L, Zhang J, Xie J, Li G. Synthesis and properties of chemically cross-linked poly(vinyl alcohol)-poly(acrylamide-co-diallyldimethylammonium chloride) (PVA-PAADDA) for anion-exchange membranes. Solid State Ionics [Internet]. 2012;214:6–12.

80. Ortega PFR, González Z, Blanco C, Lavall RL, Silva GG, Santamaría R. Biliquid Supercapacitors: a Simple and New Strategy to Enhance Energy Density in

Asymmetric/Hybrid Devices. Electrochim Acta [Internet]. 2017;254:384–92.

81. Na R, Huo P, Zhang X, Zhang S, Du Y, Zhu K, et al. A flexible solid-state supercapacitor based on a poly(aryl ether ketone)-poly(ethylene glycol) copolymer solid polymer electrolyte for high temperature applications. RSC Adv. 2016;6(69):65186–95.

82. Ni'Mah YL, Cheng MY, Cheng JH, Rick J, Hwang BJ. Solid-state polymer nanocomposite electrolyte of TiO2/PEO/NaClO4 for sodium ion batteries. J Power

83. Yang T, Liu H juan, Bai F, Wang E hui, Chen J hong, Chou KC, et al. Supercapacitor electrode based on few-layer h-BNNSs/rGO composite for wide-temperature-range operation with rob1. Yang T, Liu H juan, Bai F, Wang E hui, Chen J hong, Chou KC, et al. Supercapacitor electrode based on few-layer h-BNNSs/rGO composite for wid. Int J Miner Metall Mater. 2020;27(2):220–31.

84. Huo P, Zhang S, Zhang X, Geng Z, Luan J, Wang G. Quaternary ammonium functionalized poly(aryl ether sulfone)s as separators for supercapacitors based on activated carbon electrodes. J Memb Sci [Internet]. 2015;475:562–70.

85. Lewandowski A, Zajder M, Frackowiak E, Béguin F. Supercapacitor based on activated carbon and polyethylene oxide-KOH-H2O polymer electrolyte. Electrochim Acta. 2001;46(18):2777–80.

Appendix

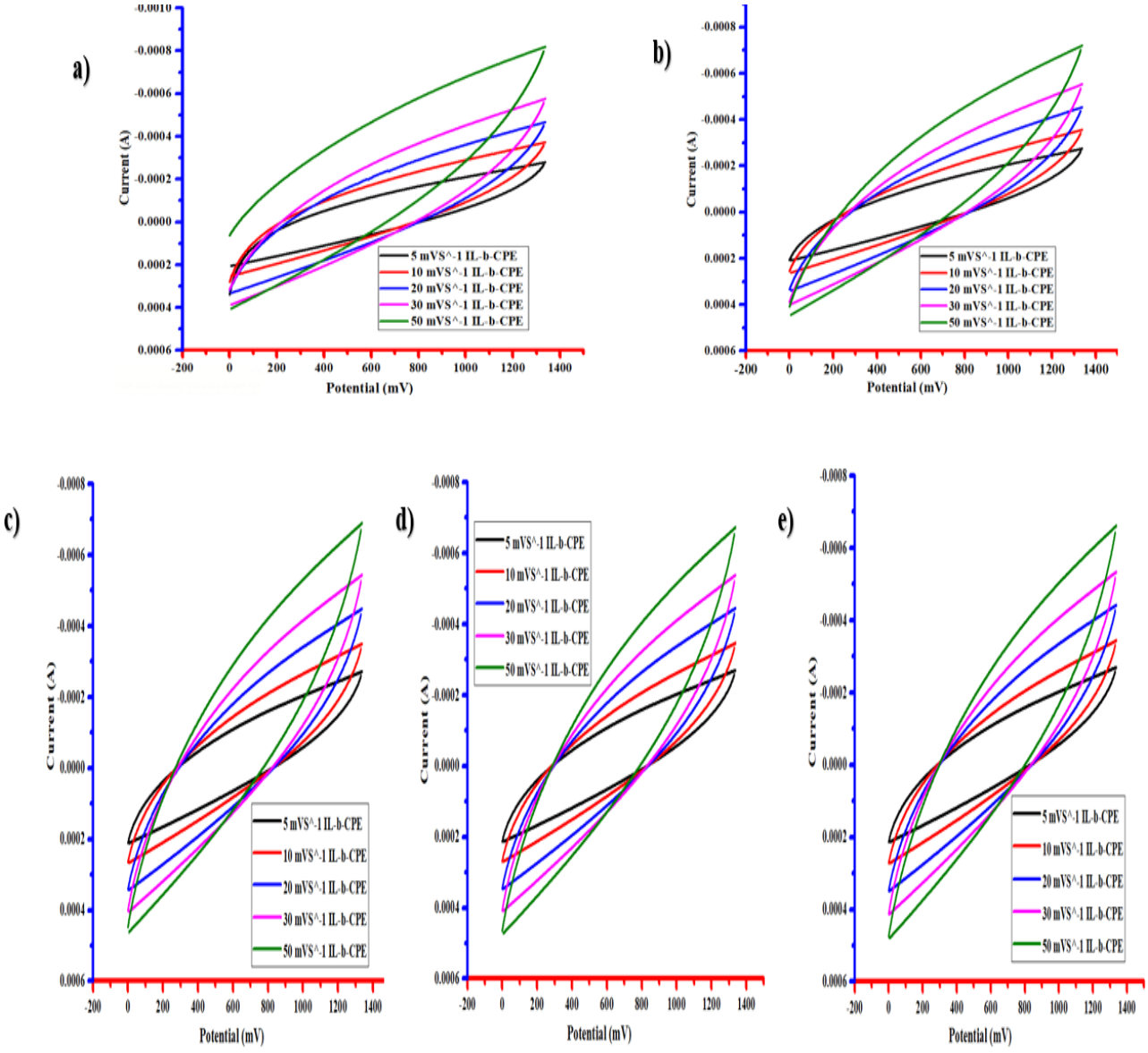

Figure 30 Different scan rat and current density of IL-b-CPE (CV)

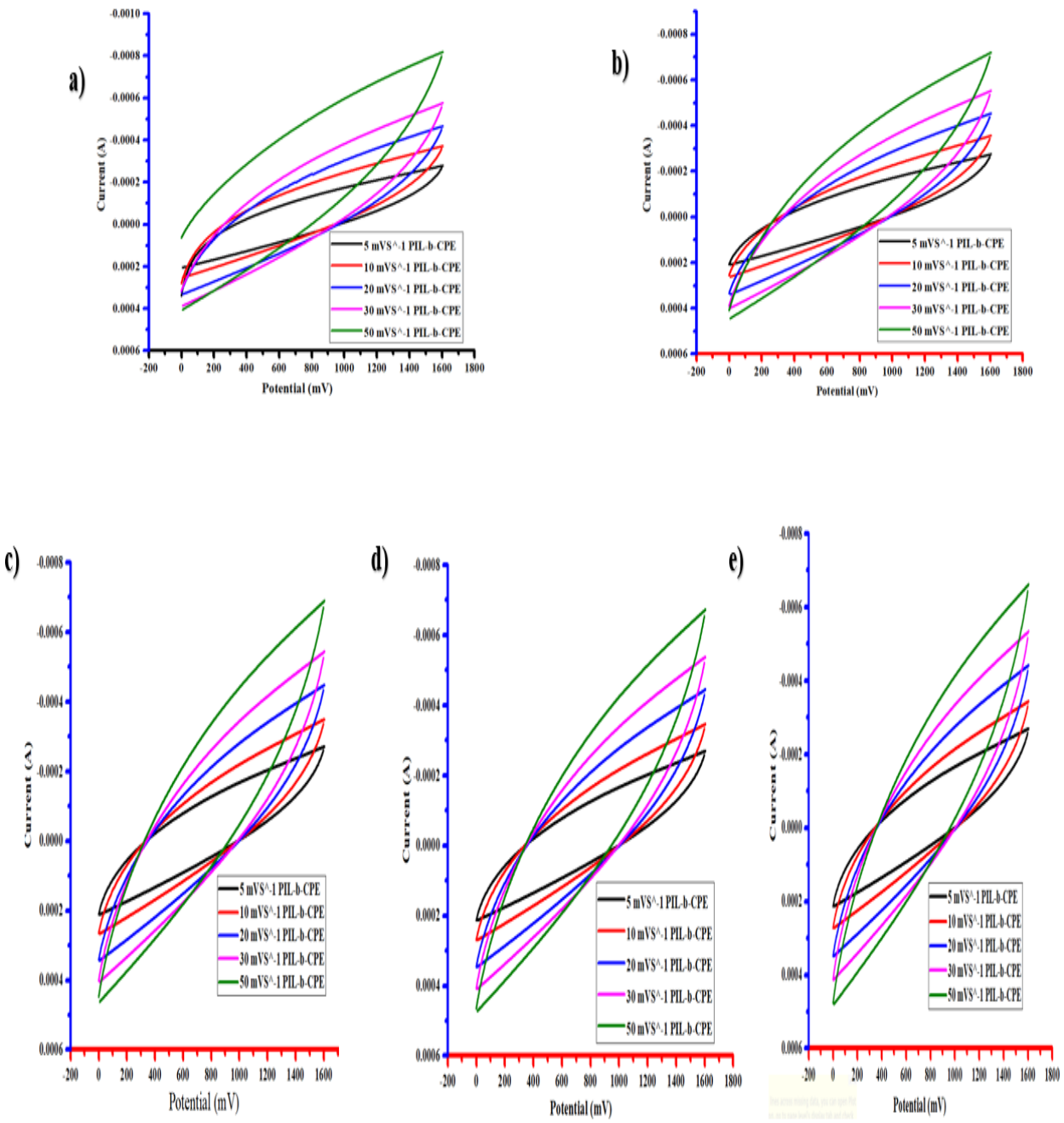

Figure 31 Different scan rat and current density of PIL-b-CPE (CV)

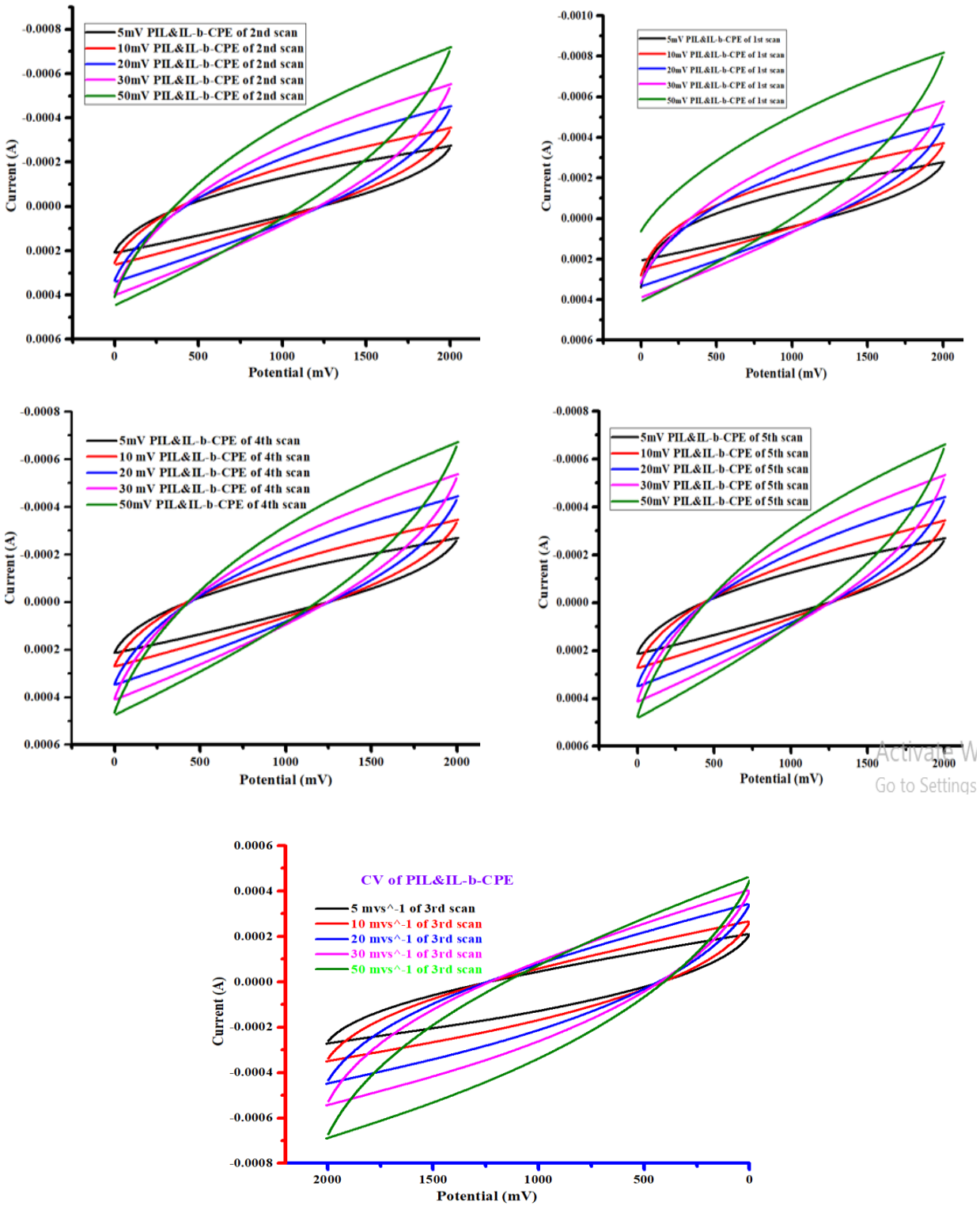

Figure 32 Different scan rat and current density of IL&PIL-b-CPE (CV)

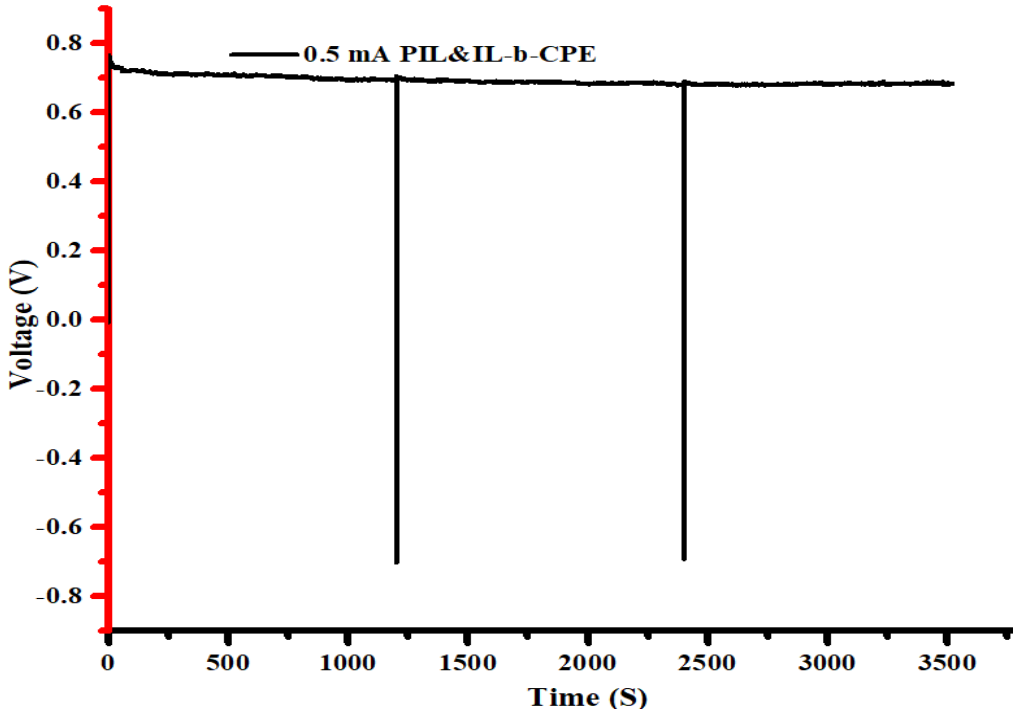

Figure *40* a) Voltage Vs time graph on the ratio of 1:0.30.

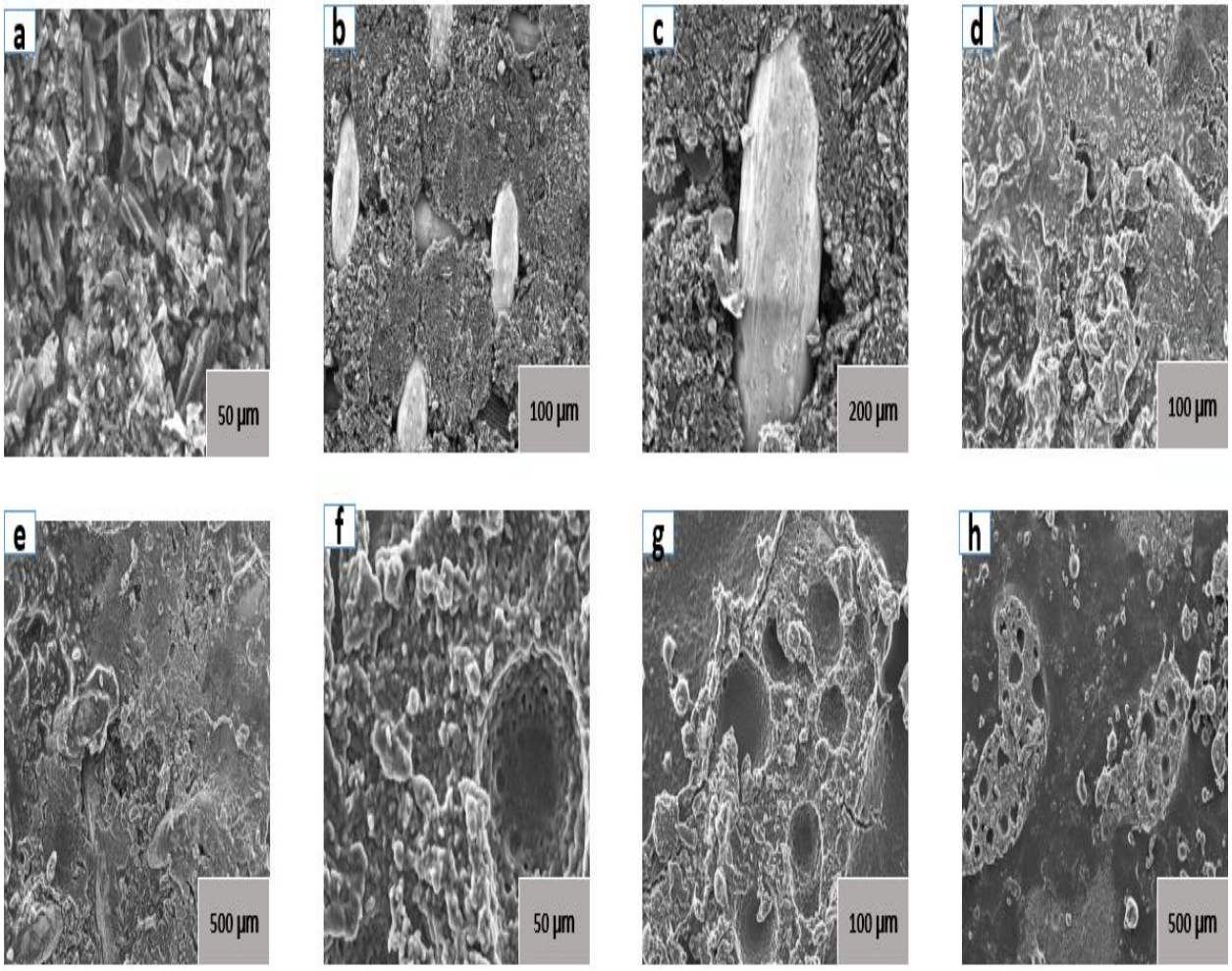

Figure 46 A-C are Carbon electrodes, D and E are polymer electrolyte with carbon electrode, and F-H are polymer electrolytes.

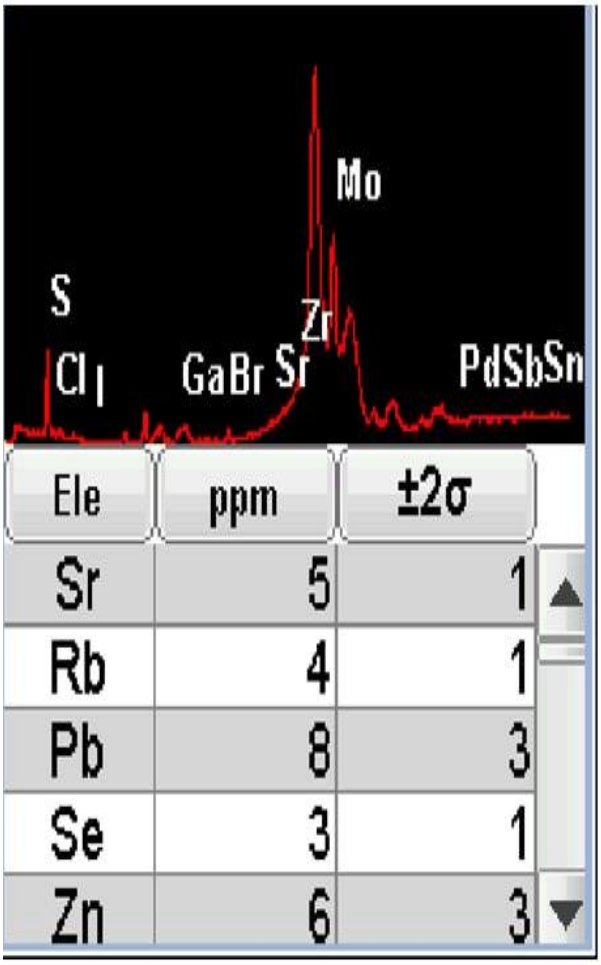

Ele	ppm	±2σ
Sr	5	1
Rb	4	1
Pb	8	3
Se	3	1
Zn	6	3

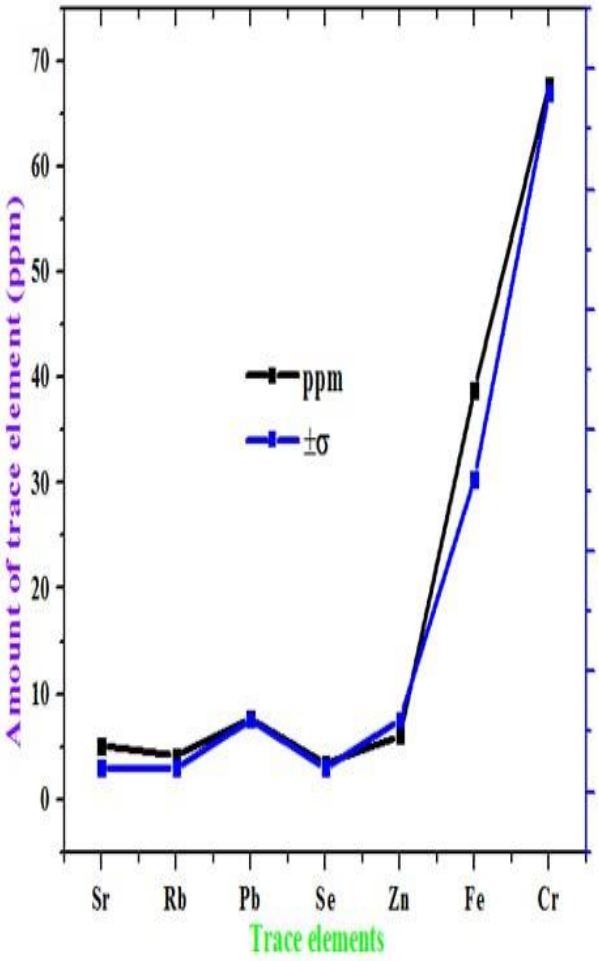

XRF image of trace elemets for copolymer electtrolyts

Copolymer Electrolyte	Current (A)	Current density (mA/cm^2)	Final voltage (Vf)	(Ir) drop (V)	Change (V)	t discharge(s)	slope (pte(mv/s))	capacitance (F/g)	Total capacitance (X4) (F/g)	ERS(Ωcm^2)	Energy density Emax (Wh/kg)	Power density Pmax (kW/Kg)	Ereal (Wh/Kg)	Preal (kW/Kg)
PIL&IL-b-CPE3														
	0.2mA	0.31	1.83	0.28	1.55	747.83	1.10	3.64	14.5455	2465.3	1.69	0.00431	0.6171	2.97
	0.3mA	0.47	2.00	0.24	1.76	306.36	2.50	2.4	9.6	1864.65	1.33	0.007	0.3801	4.466
	0.4mA	0.63	2.00	0.36	1.63	99.32	4.20	1.91	7.62	1297.76	1.06	0.01	0.1322	4.79
	0.5mA	0.79	2.00	0.34	1.67	81.68	7.20	1.39	5.56	1058.94	0.77	0.024	0.14	6.04
PIL&IL-b-CPE1														
	0.2mA	0.31	1.83	0.33	1.66	187.92	3.30	1.21	58.18	2646.72	0.56	0.01	0.125	2.40
	0.3mA	0.47	2.00	0.04	1.97	64.96	9.50	0.63	38.4	2082.97	0.35	0.0061	0.065	3.58
	0.4mA	0.63	2.00	0.09	1.91	30.72	18.10	0.44	30.47	1514.31	0.25	0.01	0.0379	4.44
	0.5mA	0.79	2.00	0.03	1.98	15.07	35.60	0.28	22.22	1256.36	0.16	0.025	0.0227	5.44
PIL&IL-b-CPE2														
	0.2mA	0.314	1.83	0.32	1.68	714.77	1.3	3.07	12.29	2670.37	1.43	0.004	0.53	0.5310
	0.3mA	0.472	2.00	0.26	1.74	272.32	3	2.00	8.01	1841.67	1.11	0.01	0.30	0.30
	0.4mA	0.629	2.00	0.2	1.80	145.79	7	1.14	4.57	1427.66	0.64	0.01	0.205	0.2054
	0.5mA	0.786	2.00	0.004	2.00	3.03	8.8	1.14	4.54	1271.54	0.63	0.01	0.0057	0.0057
PIL&IL-b-CPE4														
	0.2mA	0.42	1.83	0.348	-0.01	696.53	1.08	3.70	14.81	2356.38	1.72	0.00452	0.53	1.08
	0.3mA	0.64	2.00	0.449	0.23	272.69	2.38	2.52	10.08	1644.06	1.41	0.00648	0.30	1.61
	0.4mA	0.85	2.00	0.452	0.11	145.58	3.74	2.14	8.56	1230.66	1.19	0.01034	0.21	1.89
	0.5mA	1.06	2.00	0.636	-0.02	89.37	6.42	1.56	6.23	867.504	0.87	0.01466	0.15	1.95

Table: 3 electrochemical calculation output of solid-state copolymer electrolyte